Activation of Ano1 is Associated with Apoptosis of Pulmonary Endothelial Cells: Implications for Pulmonary Arterial Hypertension

By Ayed Allawzi

B.S., Purdue University, 2011

A Dissertation Submitted in Partial Fulfillment of the Requirements for Degree of Doctor of Philosophy in the Division of Biology and Medicine at Brown University

Providence, Rhode Island

May, 2016

This dissertation by Ayed Allawzi is accepted in its present form by the Division of Biology and Medicine as satisfying the dissertation requirement for the degree of Doctor of Philosophy.

Date:_____ Signature:_____

Gaurav Choudhary, M.D. (Advisor)

Recommended to the Graduate Council

Date:_____ Signature:_____

Anita Zimmerman, Ph.D. (Reader)

Date:_____ Signature:_____

Sharon Rounds, M.D. (Reader)

Date:_____ Signature:_____

Elizabeth Harrington, Ph.D. (Reader)

Date:_____ Signature:_____

James Sham, Ph.D. (External Reader)

Approved by the Graduate Council

Date:_____ Signature:_____

Peter M. Weber, Ph.D.
Dean of the Graduate School

Table of Contents **Page Number**

List of Tables **Page Number**

Chapter 1

Chapter 2

List of Figures **Page Number**

Chapter 1

Chapter 2

Chapter 3

List of Abbreviations (Alphabetical Order):

AVD: Apoptotic volume decrease

BMPR2: Bone Morphogenetic Protein Receptor 2

CaCC: Calcium-activated chloride channel

ECs: Endothelial cells

ESCC: Esophageal Squamous-Cell Carcinoma

ET: Endothelin

GIST: Gastrointestinal Stromal Tumor

HNSCC: Head and Neck Squamous-Cell Carcinoma

HPAECs: Human pulmonary endothelial cells

IMM: Inner mitochondrial membrane

IPAH: Idiopathic PAH

MAPK: Mitogen Activated Protein Kinases

MCT: monocrotaline

MMP: Mitochondrial membrane permeability

MOMP: Mitochondrial outer membrane permeabilization

mPAP: Mean pulmonary artery pressures

mtROS: Mitochondrial reactive oxygen species

NO: Nitric Oxide

OMM: Outer mitochondrial membrane

PAH: Pulmonary arterial hypertension

PASMCs: Pulmonary artery smooth muscle cells

PCWP: Pulmonary capillary wedge pressure

PH: Pulmonary hypertension

PVR: Pulmonary capillary wedge pressure

RLMVECs: Rat lung microvascular endothelial cells

ROS: Reactive oxygen species

SUH: Sugen hypoxia

VDAC: Voltage-dependent anion channel

VRAC: Volume-regulated anion channel

vWF: von Willebrand Factor

WSPH: World symposium on pulmonary hypertension

$\Delta\Psi m$: mitochondrial membrane potential

Contributions:

All experiments were performed by Ayed Allawzi with the exception of the following:

1. Whole cell patch clamp of RLMVECs was performed by Anlong Li, M.D. Ph.D. (Figure 3A)
2. Confocal microscopy of RLMVECs for Ano1 colocalization to mitochondria was performed by Dmitry Terentyev, Ph.D. (Figure 2A)
3. Immunofluorescence of Ano1 in intact RLMVECs was performed by Nouaying Kue, B.S. (Figure 1C)

Abstract of "Activation of Ano1 is Associated with Apoptosis of Pulmonary Endothelial Cells: Implications for Pulmonary Arterial Hypertension", by Ayed Allawzi, Ph.D., Brown University, May 2016

Aberrant endothelial cell (EC) proliferation plays an important role in the vascular remodeling observed in Pulmonary Arterial Hypertension (PAH). Anoctamin-1 (Ano1), a calcium activated chloride channel (CaCC), has been implicated in the regulation of cell proliferation in several cancer studies.

We initially set out to confirm expression and localization of Ano1 in pulmonary ECs. Next we sought to investigate the role of altered Ano1 activity in regulating the proliferative potential of pulmonary ECs. The underlying rationale was to assess whether Ano1 could serve as a molecular target for the reversal of hyperproliferative ECs associated with PAH. The findings of this dissertation are summarized as follows:

1. Ano1 is expressed in Rat Lung Microvascular ECs (RLMVECs), Human Pulmonary Endothelial Cells (HPAECs), isolated control and IPAH patient ECs. Additionally, we utilized a rat model of PAH known as Sugen-Hypoxia (SUH). We demonstrated that Ano1 levels are elevated in isolated ECs from lungs of SUH rats when compared to controls. In line with this finding, we also demonstrate that Ano1 levels in lung ECs from patients with PAH are increased when compared to lung ECs from control patients. This is the first study identifying Ano1 expression in pulmonary ECs and that Ano1 is increased in settings of PAH.
2. Ano1 is localized to the membranous and mitochondrial fractions of RLMVECs. We also demonstrated that activation of Ano1 resulted in loss

of mitochondrial membrane potential ($\Delta\Psi m$) and increased mitochondrial ROS (mtROS).

3. Activation of Ano1 resulted in p38-dependent apoptosis and caspase-3 activation. Activation of Ano1 with Eact, a small molecule activator, resulted in caspase-3 activation, mediated by increased mtROS and p38 phosphorylation.
4. Activation of Ano1 in IPAH ECs resulted in reduced cell number when compared to control ECs. Underlying this reduction in cell number was an increase in caspase-3 cleavage when compared to control ECs. Blocking mtROS and Ano1 by using MitoTEMPO and DIDS, respectively, attenuated Eact-mediated decreases in IPAH EC number, confirming that the mechanism we established in RLMVEC is relevant in lung ECs from IPAH patients as well.

Chapter 1

Background and Introduction

Pulmonary Hypertension

Pulmonary Hypertension (PH) is a progressive disease characterized by elevated mean pulmonary artery (PA) pressures (mPAP) of 25 mmHg or more at rest (1, 2). Normal physiological values of mPAP range within 8-18 mmHg (1, 2). One of the first documentations of PH can be traced to Julius Klob, a German physician who upon autopsy of a 59 year old patient presenting edema and dyspnea, noted severe narrowing and arteriosclerosis of the pulmonary arteries (3). Similarly, in 1891 Dr. Ernst von Romberg found and characterized similar pulmonary vasculopathies but additionally noted right ventricular hypertrophy (3). Although initial descriptions of PH have long been documented, more robust clinical and hemodynamic diagnosis began in the latter half of the 20th century.

By 1957, PH was already accepted as a pathophysiological disorder and was classified as either primary or secondary PH depending on the underlying causes (3). However, it was not until 1973 in Geneva, Switzerland, at the first World Symposium on Pulmonary Hypertension (WSPH) conference, did the international community convene to classify what was until then a disorganized and disjointed understanding of PH (4).

The first WSPH was initiated in response to an epidemic of primary PH which was caused by the weight loss drug Aminorex fumarate (4). Primary PH was reserved for a mostly unknown and sporadic form of PH – known today as idiopathic pulmonary arterial hypertension (PAH) (4). Secondary PH was relegated to a group of heterogeneous diseases that were known to cause primary PH-like (4).

It was not until 1998 at the second WSPH in Evian, France, did experts reconvene with the purpose to re-evaluate the groups of PH (5). The primary objective of the Evian classification was to individualize, identify, and adapt previous classifications. The paradigm of the Evian classification was based on findings concerning the mechanism of pathophysiology, clinical presentation, and therapeutic options of PH (5).

Classifications of PH

Although quickly adopted by several institutions including the European Agency for Drug Evaluation and US Food and Drug Administration, the Evian classification of 1998 remained under review by PH experts in an attempt to discern and evaluate the usefulness of the classifications (3, 5, 6). By 2003 at the third WSPH in Venice, Italy, a newer and slightly revamped and individualized classification was announced (3, 5, 6).

The modifications conducted in 2003 on the Evian classification were few but necessary based on more recent understandings of the mechanistic pathophysiology of PH (5). Additionally, genetic screening was embraced in order to further individualize diagnosis of PH (5). Of the modifications made, three major topics needed to be addressed:

1. **Reclassification of pulmonary veno-occlusive disease (PVOD) and pulmonary capillary hemangiomatosis (PCH):**

PVOD and PCH were initially separated into different classifications; PCH was formerly classified under the fifth group of PH, caused by disorders directly affecting the pulmonary vasculature (5, 7, 8). PVOD on the other hand was categorized under the second group, Pulmonary Venous Hypertension (5, 7, 8). However, by 2003, it

became evident that the two disorders should be grouped together due to the increase in medial hypertrophy, formation of occlusive plexiform lesions, and more severe clinical symptoms associated with PAH (5, 7, 8).

2. Suspending the then commonly used term "primary pulmonary hypertension."

Although the term "primary PH" had been used for over a half-century, it became necessary to revise the name. The secondary PH groups were initially grouped together; yet it was clear that the group contained heterogeneous and distinctly different mechanisms of pathophysiology (4, 5). This lumping and indiscriminate classification of clinically mixed populations was counter-productive as it did not allow for grouping based on similar pathophysiological parameters or clinical management (5). With the abandonment of secondary PH, it was thus necessary to abandon primary PH. Instead sporadic primary PH became classified as an idiopathic form of PAH.

3. Genetic screening of PH and reassessment of PH risk factors

Finally, one of the most significant revisions made in 2003 was to embrace the advent of genetic testing as a tool. It was clear at the time that one of the strong associations of hereditary PAH were mutations in the Bone Morphogenetic Protein Receptor 2 (BMPR2) (2, 5–7, 9, 10). As a result, genetic screening is now widely adopted in an attempt to stratify and further understand the genetic abnormalities underlying PH.

The Venice WSPH of 2003 unveiled a new era of PH that appreciated the complexity of PH. Two more WSPH meetings were held with little modifications made

to the structure of the Venice classifications. The fourth WSPH held in Dana Point, California, was mostly focused on the development of algorithms towards approaching the treatment of PH (11, 12). While the most recent and fifth WSPH held in Nice, France, added persistent pulmonary hypertension of the newborn (PPHN) under group 1 of PH (see Table 1) (11, 13).

Although the Nice classification (Table 1) appreciated and incorporated what was known of PH, it was evident that the Nice classification was the first wave of our knowledge of PH and its complex nature. A recent statement by the American Thoracic Society was published to organize and define the gaps in knowledge about the phenotypes of PH (14). It highlights the need for robust documentation of phenotypes with a prospective outlook not only at the genomic level but also at the transcriptional, proteomic, metabolomic, and cellular level (14). These measures will help further stratify classifications into homogenous groups and thus advance our understandings of PH pathophysiology. Importantly, the long term aim of these efforts is to develop treatment guidelines and to better develop our prognosis of PH based on underlying phenotypes.

Pulmonary Arterial Hypertension

PAH, or Group 1 PH of the Nice classification, has several sub-classifications including Idiopathic PAH (IPAH) and hereditary PAH (Table 1) (15). What the sub-classifications of PAH share in common is extreme remodeling of the pulmonary bed based on histopathological findings (8). The general diagnostic criteria for PAH is the same with regards to PH; a mPAP $\geq$ 25 mmHg, pulmonary capillary wedge pressure (PCWP) < 15 mmHg, and pulmonary vascular resistance (PVR) > 3 wood units (15). The

consequence of elevated mPAP and pulmonary vascular resistance (PVR) is right ventricle hypertrophy and subsequently right heart failure (15).

In general, the pulmonary vascular bed is a high flow and low resistance bed (8). However, in settings of PAH, there is an increase in the vasoconstriction of the pulmonary vascular bed in addition to adventitial and vascular remodeling (8, 15, 16).

Histopathological changes in the remodeling correlates and explains the more severe hemodynamic measurements associated with PAH. Adventitial fibroblasts have been shown to become activated in PAH (17). Activation of adventitial fibroblasts is associated with increased proliferation of adventitial fibroblasts as well as increasing the inflammatory recruitment to the vascular bed (17). Medial hypertrophy is documented to occur in PAH and is a consequence of pulmonary artery smooth muscle cell (PASMC) proliferation. Occlusive plexiform lesions are a result of the hyperproliferation of endothelial cells (ECs). The remodeling that occurs in the three aforementioned compartments is what renders PAH a severe disease.

Epidemiology of PAH

The prevalence and incidence rates of PAH vary depending on study. Data from 17 university hospitals participating in a French national registry resulted in prevalence of 15 cases/million adults while the incidence rate was 2.4 cases/million/year (18). Reports from Spain were similar with an estimated prevalence of 16 cases/million while the incidence rate was 3.7 cases/million/year (19). On the other hand, data from UK and Ireland registries reported a prevalence of 6.6 cases/million and an incidence rate of 1.1 cases/million/year (20). Overall, these reports suggest that PAH is a rare disease.

It has been accepted that PAH is a disease which occurs predominately in females, with 64-75% of PAH patients being females (21). With regards to age, the Registry to Evaluate Early And Long-term PAH (REVEAL), a US based multicenter registry enrolling traditional group 1 PAH, has reported that age of enrollment was 53±15 years of age (21). In support of this, the French, Spain, and UK/Ireland registries have also reported similar findings with age of enrollment occurring between the 4^{th}-5^{th} decade of age (21).

Pathogenesis of PAH

There are three primary effectors of PAH: vasoconstriction of the pulmonary vasculature, increased inflammatory recruitment, and remodeling of the adventitia and vascular bed (8, 15, 16).

Imbalanced Vasoconstriction and Vasodilation in PAH

Reductions in levels of prostacyclin and increased levels of thromboxane A_2, a potent vasodilator and vasoconstrictor, respectively, have been documented in settings of PAH (22–24). In addition, endothelin (ET), another potent vasoconstrictor, is increased in plasma from PAH patients (25, 26). Furthermore, nitric oxide (NO), a vasodilator, is reduced in patients with PAH along with reduced levels of endothelial constitutive NO synthase (eNOS), which is responsible for the synthesis and production of NO (27–29).

Finally, and perhaps most controversial, was the role of serotonin in the pathogenesis of PAH whereby it was documented that PAH patients had higher levels of serotonin (30–33). Serotonin inhibitors which increase levels of circulating serotonin was protective against PAH (30). This discordance was later explained by findings

demonstrating the presence of mutations in the serotonin receptors and increased expression of serotonin transporters amongst PAH patients (31, 32, 34). These results suggested that perhaps absolute levels of circulating serotonin are not a determinant in PAH pathogenesis but instead dysfunctional serotonin trafficking and signaling could contribute to the pathogenesis of PAH (31, 32, 34).

In summary, there is an overall increase in thromboxane A_2, endothelin, and dysfunctional serotonin trafficking that contribute to the vasoconstriction of the pulmonary bed. On the other hand, there is a reduction in available NO and prostacyclin that act as vasodilators. Together, this promotes a constricted pulmonary vascular bed contributing to increased mPAP.

Inflammation in PAH

Inflammation in settings of PAH has long been debated, due to contradictory findings in several animal models of PAH and the lack of robust human results that could associate inflammation as a possible mediator of PAH (35). However, more recent histopathological assessment demonstrates increases in T cell, B cell, and macrophage infiltrates perivascularly and at the sites of plexiform lesions (36–39). In addition to increased histological evidence, circulating levels of IL-1β, IL-2, IL-4, IL-6, IL-8, IL-10, IL-18, and TNF-α have been reported to be significantly increased in serum levels of PAH patients (35, 40, 41).

However, unlike other severe pulmonary disorders such as acute respiratory distress syndrome where strong inflammatory insults are present, it remains unclear what triggers a pro-inflammatory switch in PAH. Additionally, it is unclear whether

inflammation assists in the direct pathogenesis of PAH or whether inflammation is a reactive response to the remodeling that occurs (35). There has been some evidence to suggest that external triggers such as virus infections (herpes or HIV-associated PAH), toxins (Aminorex fumarate), and parasitic infection (Schistosomiasis-associated PAH) could be underlying causes of increased inflammation in PAH (35).

The adventitial fibroblasts have also been hypothesized to play a role in increasing the inflammatory response. Activation of adventitial fibroblasts has been shown to occur in response to hypoxia, TNFα, IL-1β, and ET-1 (17). Following activation, adventitial fibroblasts have been shown to increase inflammatory recruitment by increasing adhesion molecule expression, chemokine, and cytokine production (17). Activated adventitial fibroblasts from animal models have demonstrated increased ICAM-1 and VCAM-1 expression and thus promoting perivascular leukocyte adhesion (42, 43). Additionally, activated adventitial fibroblasts have been shown to increase TGFβ, MCP-1, and IL-1β, all of which contribute to augmenting a persistent inflammatory presence in the adventitia while exerting pro-proliferative effects as well (42, 43).

In brief, it is evident that inflammation does play an integral role in the pathogenesis of PAH. Increases in perivascular inflammatory infiltrate occur in PAH along with increases in circulating inflammatory cytokines. This shift towards an inflammatory state has been associated with promoting dysregulated metabolism and stimulating further injury to the vasculature (44). In addition, it has also been linked to the increased proliferation of adventitial fibroblasts, SMCs, and ECs (17, 44).

Dysregulated Vascular Proliferation PAH

One of the established pathologies associated with PAH is a dysregulated and hyperproliferative vascular bed, which in turn contributes to the increase in PVR and worsening of PAH (6, 8). In support of this, a three-dimensional reconstruction of vessels from PAH patients, including vessels that had plexiform lesions, demonstrated that PASMC and EC proliferation occur throughout the pulmonary vasculature (45). Ultimately, this proliferation results in narrowing of the lumen until occlusive plexiform lesions form (45).

Although this study reiterated what was already known with regards to increased vascular remodeling, it was the aberrant endothelial staining at the sites of plexiform lesions that was noteworthy (45). The authors performed staining using von Willebrand Factor (VWF) and VEGF Receptor 2 (VEGFR-2) as markers for endothelial cells. They also utilized p27/kip1 staining as a marker for quiescence. p27/kip1 stained in the periphery of the plexiform lesions and was found to be lacking at the core of the plexiform lesions (45). This suggested that the core of plexiform lesions contain cells that actively proliferate (45).

In support of the role of proliferation in PAH, a rodent animal model known as Sugen Hypoxia (SUH) has been shown to mimic a PAH-like phenotype with increased pressures and plexiform-like lesions. In this model, rodents are injected with the VEGF-R antagonist compound SU5416 and subjected to hypoxia (46). SU5416 and hypoxia are hypothesized to result in injury and apoptosis of ECs early on. Following this insult, anti-apoptotic ECs, which are hyperproliferative in phenotype, begin to proliferate into the lumen in setting of hypoxia. As a result, rodent SUH animals exhibit a phenotype of extensive vascular remodeling and the formation of plexiform-like lesions; the formation

of plexiform-like lesions in this model is a fundamental difference between previous rodent models of PH (46).

Proliferation of PASMC and ECs in PAH has been shown to be mediated by several regulators. As mentioned earlier, overall levels of NO are reduced in PAH patients; however, reports have also shown that NO levels are increased at the sites of plexiform lesions. It has been postulated that NO at sites of plexiform lesions plays a role in increasing proliferation due to NO having mitogenic properties as well (27–29).

Similarly, increases in ET production by the pulmonary vascular endothelium has been shown to act in paracrine fashion to increase the proliferation of PASMCs and ECs (47). ET increases proliferation via ET-A and ET-B receptors that are expressed in PASMCs and ECs (26, 47, 48). Mechanistically, ET has been shown to exert its mitogenic properties by increasing phosphorylation and levels of c-fos, a proto-oncogene often seen upregulated in PAH patients, and ET-dependent Erk1/2 phosphorylation (49).

Serotonin, another vasoconstrictor that plays a role in PAH, has also been implicated in increasing PASMC proliferation (32, 33). Serotonin was found to be increased not only in platelets as originally hypothesized, but also to be increased in PASMCs (31, 32). Furthermore, mutations in the serotonin transporter have been linked to increasing PASMC proliferative potential (31). Recent evidence has shown that serotonin-induced proliferation is mediated via increased Erk1/2 activity (50, 51).

On the other hand, mutations in BMPR2, a member of the TGF-β family, has been highly associated with PAH, with an estimated 30% of PAH patients having some form of mutation in the BMPR2 gene (52). In addition, PAH patients with BMPR2

mutations often have worse outcomes in addition to more severe hemodynamic changes (52).

The role of BMPR2 in the remodeling of the pulmonary vascular bed is two-fold; decreased BMPR2 signaling, due to mutations in the gene or knockdown, has been shown to increase apoptosis of ECs while simultaneously increasing PASMC proliferation (53, 54). This divergence in roles can be explained that early EC apoptosis is hypothesized as trigger in the pathogenesis of PAH, resulting in an apoptotic-resistant and pro-proliferative endothelium (52, 54).

Mechanistically, the BMPR2 receptor mediates much of its effects through downstream signaling via SMAD1/5/9 (55). TGF-β, on the other hand mediates signaling events via SMAD2/3 (54, 56). Active BMPR2 signaling exerts anti-proliferative and pro-apoptotic effects that balance the pro-proliferative and anti-apoptotic signaling of TGF-β (54, 56). As a result, dysfunctional BMRP2, as is the case in PAH, shifts the balance in favor of TGF-β signaling, thus, promoting proliferation.

Other genetic abnormalities related to dysfunctional TGF-β signaling have also been reported in PAH. Mutations in ALK-1 and SMAD9, which are members of the TGF-β superfamily signaling cascade, have been identified in a small percentage of hereditary PAH patients (55). Similar to BMPR2 mutations, mutations in ALK-1 and SMAD9 shift the balance in favor of TGF-β resulting in further proliferation of PASMCs (56).

Other heritable mutations have also been associated to regulation of proliferation in PAH as well. KCNK3, a potassium channel, has been found to be decreased in patients

with IPAH and hereditary PAH (57). Recent evidence suggests a loss of KCNK3 can increase both EC and PASMC proliferation by increasing ERK1/2 activity and remodeling by increased vimentin production (57). Also, mutations in Cav1 have been linked to decreased NO production, but more importantly, increase pro-proliferative ERK1/2 activity (55). Cav1 has also been shown to dampen BMPR2 signaling, thus, increasing proliferation by favoring TGF-β signaling (55).

There has also been evidence to suggest that ECs from PAH undergo a phenotypic switch. Cultured ECs from PAH patients maintain proliferation while serum deprived, display increased migration, and have poorer tube formation (58). Mechanistically, PAH ECs were also shown to have decreased caspase-3 activity, increased Bcl-2 (anti-apoptotic), increased MCl-1 (anti-apoptotic), and increased STAT3 (pro-proliferative) (58). This anti-apoptotic shift in PAH ECs in the midst of pro-proliferative mediators has been suggested to underlie the hyperproliferation associated with PAH ECs (58).

Metabolically, pulmonary ECs from PAH patients favor ATP generation using a glycolytic pathway with lower rates of oxygen consumption as a source of energy, also known as the Warburg effect (59). The Warburg effect provides rapidly proliferating cells with the essential building blocks by increasing glucose uptake (59, 60). To explain this, the authors showed an overall decreased mitochondria content; additionally, there is a decrease in complex IV activity, which is the last step in ATP generation (59). Others have also shown that the mitochondria in PAH is significantly hyperpolarized as well (61). This suggests another mechanism by which an anti-apoptotic phenotype is consequential, where mitochondrial depolarization is required for apoptosis to ensue (62).

In summary, the pathogenesis of PAH is clearly complex. Underlying this complicated disorder is a transofrmation towards a chronically inflammed, constricted, and remodeled vascular bed. A neoplastic shift occurs where PASMCs and ECs become pro-proliferative and anti-apoptotic in phenotype resulting in increased PVR and ultimately mPAP. Although our understanding of PAH pathogenesis has increased over the years leading to approved medications for PAH, few are capable of targeting the hyperproliferation or reversing the extensive vascular remodeling that occurs in PAH.

Apoptosis: A Role for Ion Channels

Apoptosis: Extrinsic and Intrinsic Pathways

Apoptosis is one of the multiple forms of programmed cell death mechanisms (63). Tightly controlled, apoptosis can be initiated by extrinsic and/or intrinsic factors and ends in the activation of effector proteases caspase-3, -6, or -7 (63). After activation of effector caspases, apoptosis results in a series of subsequent changes that allow for cell death to proceed; these include endonuclease activation that degrades chromosomal DNA, further protease activation that degrades proteins allowing for cytoskeletal reorganization, and morphological changes mediated by cytoplasmic and chromatin condensation (63).

Although the series of steps after the recruitment of the effector caspases is tightly regulated and well understood, variability in achieving cell death occurs upstream where multiple cell stressors can induce apoptosis. The extrinsic pathway induces apoptosis by binding of external ligands to a receptor which in turn signals for apoptosis (63). Of the

most well-characterized mediators of extrinsic apoptosis are receptors of the TNF superfamily that contain a cytoplasmic death-domain (63). The death-domain mediates apoptotic signaling intracellularly by the formation of a death-inducing signaling complex (DISC) (63). The formation of the DISC results in the recruitment of caspase-8, an initiator caspase, that activates caspase-3 (63).

The intrinsic pathway differs from the extrinsic due to the lack of transmembrane receptor-mediated signaling. Examples of intrinsic signals are UV, radiation, hypoxia, serum starvation, heat shock, cell swelling, intracellular acidosis, and reactive oxygen species (ROS) (63, 64). These initial signals converge by causing alterations in the mitochondria that cause mitochondrial membrane permeability (MMP) and, thus, loss of the highly hyperpolarized and regulated mitochondrial membrane potential ($\Delta\Psi m$) (63). This loss of $\Delta\Psi m$ and the opening of the MMP result in the release of mitochondrial apoptogenic proteins such as cytochrome c, SMAC, or HtrA2 (63). The release of apoptogenic proteins results in the recruitment of initiator caspases (caspase-2, -8, -9, and -10) that then activate executor caspases (63). However, there has also been evidence to support the release of apoptogenic proteins that do not act via the caspase pathway directly. These caspase-independent effectors include AIF and endonuclease G, which participate in the process of apoptosis by causing fragmentation of DNA independent of caspases (65).

The BCL-2 family of proteins play an integral role in mediating intrinsic apoptosis by regulating the mitochondrial outer membrane permeabilization (MOMP). The BCL-2 family can be divided into anti-apoptotic (Bcl-2, Bcl-X_L, Mcl-1, Bcl10, and Bfl1) and pro-apoptotic (Bid, Bad, Bik, Bim, Bax, Bak, and Bok) (66). The

aforementioned regulators act in concert and balance apoptosis. Upon triggering of apoptosis via the intrinsic pathway, the inhibitory effect of anti-apoptotic members is relieved and the pro-apoptotic members activate to form a pore (66). As a result, MOMP ensues and release of mitochondrial apoptogenic proteins occurs, triggering apoptosis (66).

Notably, the intrinsic pathway can result in apoptosis by two different mechanisms of altering mitochondrial function. Firstly, MMP can occur due to disruption of the OMM mediated by MOMP where members of the BCL-2 family converge and form pores allowing the release of apoptogenic proteins into the cytosol (65). On the other hand, stressors such as Ca^{2+} overload cause alterations in IMM whereby a permeability transition pore complex is formed which allows the release of apoptogenic proteins (65). In both cases, a persistent theme of $\Delta\Psi m$ depolarization, release of apoptogenic proteins, and recruitment of effector caspases occurs to induce apoptosis (65).

ROS, including mtROS, has been shown to promote apoptosis in several fashion. ROS has been shown to directly activate VDAC and ANT, which promotes pore formation and thus MMP (67). In addition, ROS has also been show to activate stress MAPKs, including p38, Jnk, and the oncogene p53 (67, 68). In return, they act to phosphorylate anti-apoptotic members of the BCL-2 family, relieving inhibition of apoptosis and triggering of MOMP (67).

Ion Channels: Regulators of Apoptosis

From the initial identification of ion channels as proteins capable of conducting ions and currents, their role in regulating cell proliferation has expanded. Though the initial link between ion channels and apoptosis remained unclear, it is now established that ion channels can cause apoptosis via downstream signaling to members of the Mitogen-Activated Protein Kinases (MAPK) family. More specifically, several ion channels have been shown to mediate apoptosis via p38, p53, and JNK (69). These "stress" sensing MAPKs are capable of sensing intrinsic signals mediated by ion channels, such as cell volume alterations or increases in ROS and trigger apoptosis (69).

Calcium Channels

Sustained intracellular Ca^{2+} can cause apoptosis through several pathways. Cytosolic overload of Ca^{2+} results in increased Ca^{2+} uptake into the hyperpolarized mitochondria, resulting in triggering MMP and apoptosis (70–73). Another mechanism by which Ca^{2+} can cause apoptosis is through binding to members of the calpain family that regulate cleavage of BCL-2 family members (Bid, Bcl-2, and Bcl-X_L) (74, 75). Furthermore, Ca^{2+} can activate calcineurin, which in turn is capable of dephosphorylating Bad resulting in increased apoptosis by dimerization with Bcl-X_L (76).

Inositol 1,4,5-triphosphate Receptor (IP_3R) is localized to the endoplasmic reticulum that serves as the largest store of intracellular Ca^{2+}. The opening of IP_3R can trigger apoptosis simply due to its proximity to the mitochondria where it promotes Ca^{2+} uptake into the mitochondria (77). Also, IP_3R can be cleaved by calpain or caspase-3 to enhance further Ca^{2+} uptake into the mitochondria (78, 79). In a similar fashion, the

Mitochondrial Calcium Uniporter (MCU) and VDAC, which are present in the inner mitochondrial (IMM) and outer mitochondrial membrane (OMM), respectively, are capable of mediating increased calcium uptake into the mitochondria resulting in MMP.

Members of the TRP superfamily have also been implicated in inducing apoptosis. TRPM8, when inhibited, causes apoptosis of prostate cancer cell line LNCaP (80). Conflicting findings were documented where both activation and silencing of TRPM8 were shown to cause apoptosis (81, 82). In line with these paradoxical finding, TRPV1 has also resulted in conflicting findings depending on cancer cell type, with both activation and silencing resulting in increased apoptosis mediated via alteration in the intrinsic pathway (83, 84). These conflicting results provide evidence that ion channels can exert apoptotic effects in a cell-specific manner.

Potassium Channels

Unlike Ca^{2+}, which can mediate apoptosis directly through the intrinsic pathway via uptake into the mitochondria, K^+ was historically known to cause apoptosis through changes in volume (64). Upon opening of K^+-channels, K^+ efflux follows and results in cell shrinkage, also known as Apoptotic Volume Decrease (AVD).

Kv2.1 has been shown to induce apoptosis by increasing cellular ROS (85). On the other hand, IK channels have been shown to cause apoptosis by increasing driving force for Ca^{2+} entry resulting in Ca^{2+} overload of mitochondria (86). Recent evidence demonstrates a few mitochondria-localized K^+-channels, including BK_{Ca}, IK_{Ca}, Kv1.3, K_{ir}, K_{ATP}, and TASK3 (87). Disruption of these channels can cause apoptosis by dysregulating mitochondrial volume, ROS production, and generation of ATP (87).

Chloride Channels

In similar fashion to K^+-channels, Cl^-, which is abundant intracellularly in several cell types, can result in triggering apoptosis via AVD. Volume-Regulated Anion Channel (VRAC), which is ubiquitously expressed, has been shown to cause apoptosis by inducing AVD (88). Molecular candidates for VRAC are still widely debated. However, two candidates for VRAC to date are ClC-2 and ClC-3 (64).

Inhibition of CFTR activity has been shown to blunt induction of apoptosis suggesting a possible role for CFTR in apoptosis (89). In support of this, increases in CFTR expression has been shown to cause apoptosis by altering the activity of Cl^-/HCO_3^- that resulted in intracellular acidification (90). In contrast, when overexpression of CLIC4, a mitochondrial localized channel, has been shown to cause apoptosis in a p53-dependent manner where it has been suggested to modulate mitochondrial pH and ATP generation (91).

In summary, ion channels can mediate apoptosis through various mechanisms. Ca^{2+}-channels are capable of directly causing apoptosis by increasing Ca^{2+} overload of the mitochondria or by modulation of anti-apoptotic and pro-apoptotic proteins. K^+ and Cl^--channels have both been shown to mediate apoptosis by AVD, alterations of intracellular pH, and modulation of mitochondrial function.

A class of chloride channels known as calcium-activated chloride channels (CaCC) were discovered over three decades ago (92). Based on electrophysiological studies, CaCC currents were detected in several cell types (93). However, their physiological function remained unclear due to a lack of any molecular candidates or the

availability of specific activators or inhibitors. It not known whether altering CaCC activity or expression would result in apoptosis.

Calcium-Activated Chloride Channels: Anoctamin-1

In 1982, two independent groups identified what they described as CaCC that were capable of conducting chloride in Xenopus oocytes and salamander retina (94, 95). Since their initial findings, these channels were expanded upon and identified in several cell types including pulmonary and vascular smooth muscle cells and endothelial cells. However, for over 30 years the molecular candidates for CaCC remained elusive. Various channels were suggested to mediate these currents including members of the ClC, CLIC, and bestrophin channels as possible candidates (93). However, with time each and every candidate failed to fit the electrophysiological characteristics of CaCC. In 2008, three independent groups identified Ano1 (also known as TMEM16A) as the long elusive CaCC (96–98).

Biophysical Properties of Ano1

While the three landmark papers that identified Ano1 as the molecular candidate for CaCC did so using various expression profiling techniques for Ano1, all three groups reported almost identical biophysical properties (96–98). All three groups observed a strong outward rectifying current at low concentrations of calcium but upon increasing calcium the I-V curve shifted towards a linear relation (96–98). This essentially suggests that Ano1, like CaCC at low doses of calcium, can conduct current at depolarized

membrane potentials but upon increasing calcium can conduct current regardless of membrane potential.

Next, anion permeability was assessed whereby Ano1 mirrored the established CaCC permeability profile, and Ano1 favored larger anion entry ($I^->Br^->Cl^->F^-$) (97, 98). Ano1 sensitivity to chemical inhibitors also mirrored CaCC, with Ano1 being more sensitive to DIDS (4,4'-Diisothiocyano-2,2'-stilbenedisulfonic acid) and NFA (2-{[3-(trifluoromethyl)phenyl]amino}nicotinic acid) than NPPB (5-nitro-2-(3-phenylpropyl-amino) benzoic acid) (97, 98).

Ano1 also matched the profile of CaCC concerning Ca^{2+} sensitivity. Ano1 at negative holding potentials (-60mV) displayed an EC_{50} for activation in a low micromolar range (2.6 μM) but positive holding potentials (+60mV) shifted the EC_{50} as Ano1 became more sensitive to calcium (400 nM) (97). Ano1 currents also became inactivated upon the use of supraphysiological concentrations of calcium (greater than 10μM), mirroring CaCC properties (97).

Ano1 in Cancer

After the cloning of Ano1, an unexpected result was the finding that Ano1 was molecularly identical to that of DOG1 (Discovered on Gastrointestinal Stromal Tumor 1), TAOS2 (Tumor Amplified and Overexpressed Sequence 2), ORAOV2 (Oral Cancer Overexpressed 2) (99). As the names suggest, subsequent studies emerged tying Ano1 to roles implicated in cancer such as cell proliferation, migration, and tumor invasiveness.

Ano1 overexpression has been linked to a vast majority of cancer cell lines including ESCC (Esophageal Squamous-Cell Carcinoma), HNSCC (Head and Neck Squamous-Cell Carcinoma), GIST, pancreas, breast, and prostate cancer (99).

Overexpression of Ano1 in T24 cells (bladder carcinoma), which do not endogenously overexpress Ano1, resulted in augmenting cell proliferation (100). One of study demonstrated that Ano1 protein and mRNA levels were significantly increased in tumors from HNSCC patients, and Ano1 expression levels correlated with overall decreased patient survival (101). Using HNSCC tumor xenografts, the authors demonstrated that Ano1 knockdown reduced tumor growth while overexpression in T24 tumor xenografts increased tumor size via ERK1/2 activation (101).

Ano1 was also shown to play a significant role in breast cancer, whereby Ano1 levels were elevated in patients and was a predictor of survival (102). Similar to previous findings, Ano1 mediated these effects by increasing EGFR, CAMKII, and ERK1/2 activity (102). In LNCaP and PC3 cells (prostate cancer), Ano1 levels and currents were also increased (103). PC3 tumor xenografts induced an increase in tumor growth as expected. However, knockdown of Ano1 in PC3 reversed tumor growth cells decreased cell viability (103). Also, the authors showed that knockdown decreased cell migration and invasiveness measured by scratch and Matrigel transwell assays (103).

However, further studies have provided conflicting evidence when compared to earlier studies due to absence of data supporting Ano1 as a mediator of proliferation. Knockdown of Ano1 in BHY cells, a type of HNSCC cell line that overexpresses Ano1, reduced migration while knockdown caused no changes in proliferation (104).

Overexpression of Ano1 in HEp-2, also a HNSCC cell line, did not increase proliferation but was capable of increasing wound healing, cell spreading, and cell detachment (105).

Other groups have also demonstrated that Ano1 does not alter proliferative or migratory potential. Knockdown of Ano1 in GIST-T1 and GIST882 did not alter proliferation or alter cell viability as well (106). Another group has shown that overexpression of Ano1 in HEK293 cells did not alter either migration or proliferation (107).

Taken together, it is evident that Ano1 can play a role in mediating phenotypes associated with cancer such as proliferation and migration. However, perhaps Ano1 is not a strict determinant of proliferation in all settings as it was first proposed by many groups. Instead, Ano1 could regulate mitogenic properties depending on whether the environment is primed to allow Ano1 to exert pro-proliferative and pro-migratory functions. Also, if Ano1 is strictly capable of changing proliferative function in cancerous settings, it is unclear whether it can do so in non-cancerous settings.

Ano1 in the Vasculature and Lung

Since the identification of CaCC currents, many have postulated about its possible role in regulating vascular function. While there have been advances in understanding the role of chloride channels in the vasculature, CaCC remained understudied due to the lack of any molecular candidates. Although almost a decade has passed since the cloning of Ano1 and establishing its ubiquitous expression in several tissue and cell types, the role of Ano1 in the vasculature remains unclear.

One of the initial studies performed an expression profile of Ano1 localization in the smooth muscle (108). Ano1 expressed in all of the aorta, portal vein, carotid artery, and pulmonary artery as assessed by PCR (108). Additionally, CaCC currents were detected in the portal vein, thoracic aorta, and carotid artery smooth muscle cells (108). Several groups also confirmed that Ano1 was expressed in smooth muscle cells from both pulmonary artery and cerebral artery smooth muscle cells, where Ano1 currents were also present (109, 110).

In 2012, two different groups demonstrated that Ano1 levels in PASMCs were elevated using a chronic hypoxia and monocrotaline (MCT) model of PH (111, 112). Findings from both studies indicated that in addition to increased Ano1 levels, whole cell Ano1 currents were augmented as well (111, 112). Both groups reported that due to the increased levels of Ano1 expression and currents, pulmonary artery contractility was enhanced (111, 112).

Therefore, current evidence suggests that Ano1 is ubiquitously expressed in smooth muscle cells. Increases in Ano1 expression and activity have been shown enhance vascular contractility. However, in contrast with the studies of Ano1 in cancer, little is known about the role of Ano1 in mediating proliferation of vascular cells.

Only one study to date has demonstrated the presence of Ano1 in cardiac vascular endothelial cells (CVECs) isolated from the left ventricles of neonatal mice (113). The authors show that Ano1 levels increase in CVECs following hypoxia (2% FiO_2 in culture) both at the protein and mRNA level (113). However, Ano1 inhibition did not attenuate hypoxia-induced proliferation, suggesting that perhaps Ano1 does not contribute to the proliferation associated with hypoxia (113).

In the lung, Ano1 expression is elevated in airway smooth muscle (ASM) in an ovalbumin model of asthma (114). Knockdown of Ano1 in ASM reduced spontaneous transient inward currents (114). As a result, decreased Ano1 expression decreased airway hyperresponsiveness that is associated with asthma (114). Another study demonstrated that Ano1 in airway epithelium is protective in a liposaccharide (LPS) model of acute lung injury (115). Knockdown of Ano1 alone resulted in decreased alveolar fluid clearance (115). LPS stimulation on the other hand increased levels of Ano1, resulting increased alveolar fluid clearance suggesting a protective role (115).

Over the past eight years, the role of Ano1 in cancer has grown with several studies demonstrating the role of Ano1 in the pathogenesis of some cancer types. However, the pathophysiological role of Ano1 beyond regulating contractility in the vasculature remains understudied. There are several vascular settings, such as PAH, where aberrant proliferation plays a role in the pathogenesis of the disease. Understanding the role of Ano1 in these settings is an important area of investigation.

Summary

PAH is a severe disease where EC proliferation mediates an important part of the pathogenesis of the disease. EC proliferation ultimately results in the formation of plexiform lesions in PAH. Therefore, reversing the hyperproliferation associated with PAH ECs is could serve as an important target.

Ano1 has been shown to be upregulated in various cancers and cancer cell lines, and is associated with the proliferation underlying these cancer cells. It is not known whether Ano1 is expressed in pulmonary ECs. Additionally, it is not known if Ano1

expression changes in ECs in settings of PAH. Furthermore, it is unknown whether altered activity of Ano1 in pulmonary ECs would alter proliferative functions such as proliferation, cell cycle, or cell death.

Therefore, we set out to characterize the expression of Ano1 in pulmonary ECs. We also sought to determine if Ano1 expression was altered in settings of PAH. Finally, we also determined whether Ano1 would result in altering the proliferative function of pulmonary ECs.

Table 1: Most recent clinical classifications of pulmonary hypertension following the fifth WSPH in Nice, France

Group 1	**Pulmonary Arterial Hypertension (PAH)** 1.1 Idiopathic PAH 1.2 Heritable PAH: BMPR2, ALK-1, ENG, SMAD9, CAV1, KCNK3 1.3 Drug or toxin induced 1.4 PAH associated with: 1.4.1: Connective tissue disease 1.4.2: HIV 1.4.3: Portal hypertension 1.4.4: Congenital heart disease 1.4.5: Schistosomiasis 1' Pulmonary veno-occlusive disease (PVOD) or pulmonary capillary hemangiomatosis (PCH) 1'' Persistent pulmonary hypertension of newborns (PPHN)
Group 2	**Pulmonary hypertension due to left heart diseases** 2.1 Left ventricular systolic dysfunction 2.2 Left ventricular diastolic dysfunction 2.3 Valvular disease 2.4 Congenital or acquired left heart inflow/outflow tract obstruction and congenital cardiomyopathies
Group 3	**Pulmonary hypertension due to chronic lung disease or hypoxia** 3.1: Chronic obstructive pulmonary disease 3.2: Interstitial lung disease 3.3: Other pulmonary disease with mixed restrictive and obstructive pattern 3.4: Sleep-disordered breathing 3.5: Alveolar hypoventilation disorders 3.6: Chronic exposure to high altitudes 3.7: Developmental lung diseases
Group 4	**Chronic thromboembolic pulmonary hypertension**
Group 5	**Pulmonary hypertension due to unclear multifactorial mechanisms**

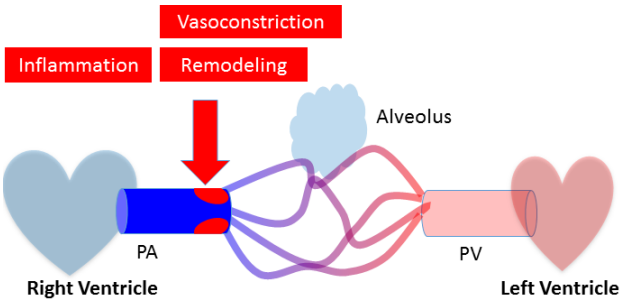

Figure 1: Several players contribute in the pathogenesis of PAH. Increases in inflammation, vasoconstriction, and remodeling occur at the distal branches of the pulmonary artery (PA).

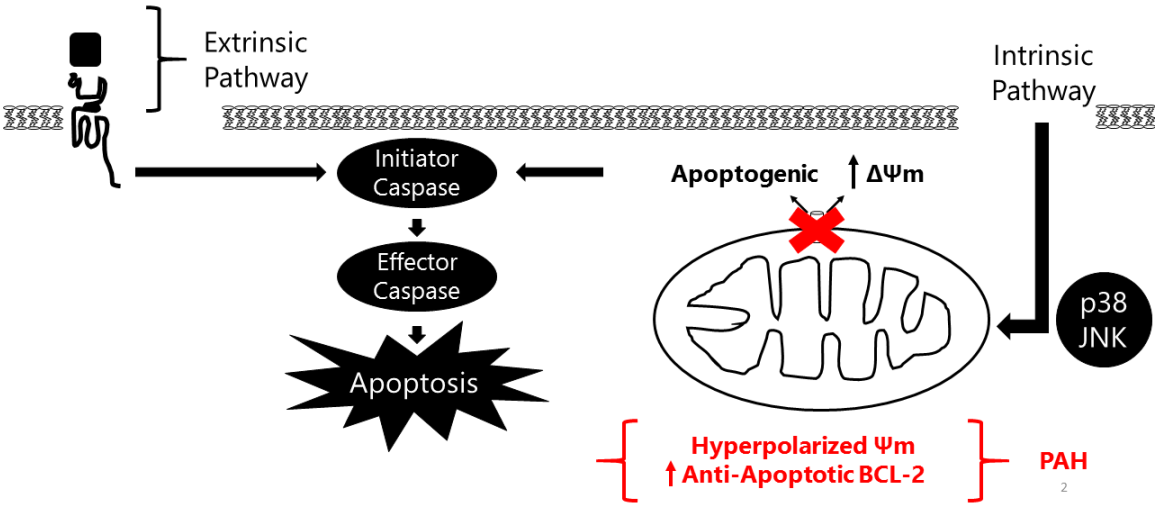

Figure 2: Apoptosis can be mediated by two common pathways, the extrinsic and intrinsic pathway. For the extrinsic pathway, the binding of an extrinsic death ligand to a death receptor mediates intracellular signaling and recruitment of initiator caspases followed by effector caspase activation allowing apoptosis to ensue. The intrinsic pathway does not require binding to any receptor, and instead signaling ultimately converges and results in alteration of mitochondrial function (release of apoptogenic proteins and ΔΨm depolarization) which signals for apoptosis by recruitment of initiator caspases that activate effector caspases. In PAH, an apoptotic resistant endothelial cell population occurs by increasing anti-apoptotic members of the BCL-2 family and altering mitochondrial membrane potential and metabolism.

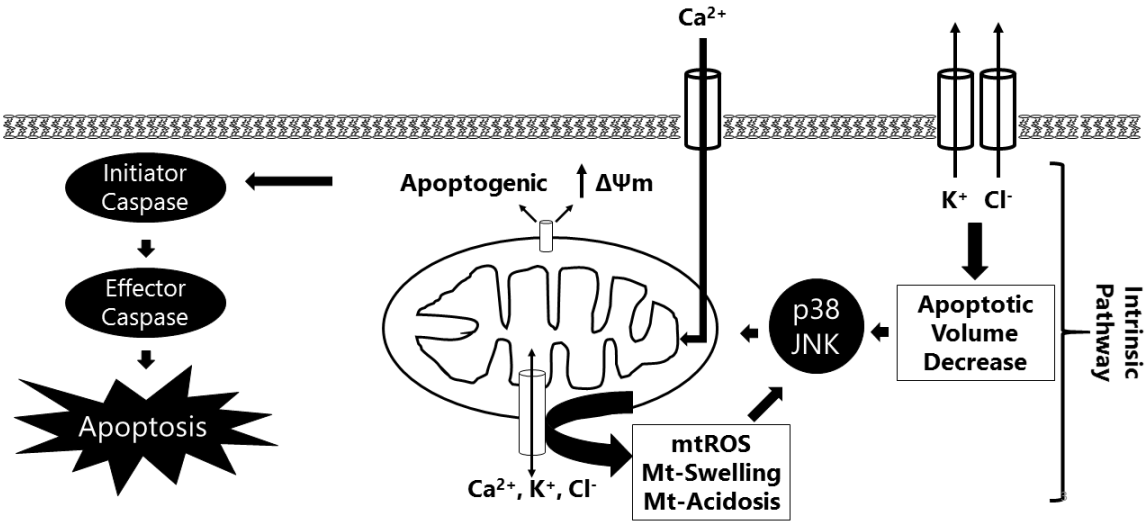

Figure 3: Ion channels mediate apoptosis predominately via the intrinsic pathway. Calcium channels have been historically shown to induce apoptosis by increasing cytosolic calcium which overloads the mitochondria. On the other hand, potassium and chloride channels have also been shown to induce apoptosis by triggering a process known as apoptotic volume decrease, which alters mitochondrial function by recruitment of stress MAPKs (p38 and JNK). Additionally, mitochondrial ion channels have been shown to be present in the mitochondria and can induce apoptosis directly by altering mitochondrial function.

References

1. Goldman L, Schafer AI, Mclaughlin V. Pulmonary Hypertension. *Goldman's Cecil Med* 2012;308:389–397.

2. Kiely DG, Elliot CA, Sabroe I, Condliffe R. Pulmonary hypertension: diagnosis and management. *Bmj* 2013;346:f2028–f2028.

3. van Wolferen SA, Grünberg K, Vonk Noordegraaf A. Diagnosis and management of pulmonary hypertension over the past 100 years. *Respir Med* 2007;101:389–398.

4. Hatano S, Strasser T, Organization WH. Primary pulmonary hypertension : report on a WHO meeting, Geneva, 15-17 October 1973 / edited by Shuichi Hatano and Toma Strasser. 1975;at <http://apps.who.int//iris/handle/10665/39094>.

5. Simonneau G, Galiè N, Rubin LJ, Langleben D, Seeger W, Domenighetti G, Gibbs S, Lebrec D, Speich R, Beghetti M, Rich S, Fishman A. Clinical classification of pulmonary hypertension. *J Am Coll Cardiol* 2004;43:S5–S12.

6. Tuder RM, Marecki JC, Richter A, Fijalkowska I, Flores S. Pathology of Pulmonary Hypertension. *Clin Chest Med* 2007;28:23–42.

7. Pietra GG, Capron F, Stewart S, Leone O, Humbert M, Robbins IM, Reid LM, Tuder RM. Pathologic assessment of vasculopathies in pulmonary hypertension. *J Am Coll Cardiol* 2004;43.:

8. Tuder RM, Stacher E, Robinson J, Kumar R, Graham BB. Pathology of pulmonary hypertension. *Clin Chest Med* 2013;34:639–650.

9. Bull TM, Coldren CD, Geraci MW, Voelkel NF. Gene expression profiling in pulmonary hypertension. *Proc Am Thorac Soc* 2007;4:117–120.

10. Tuder RM, Abman SH, Braun T, Capron F, Stevens T, Thistlethwaite PA, Haworth SG. Development and Pathology of Pulmonary Hypertension. *J Am Coll Cardiol* 2009;54:S3–9.

11. Gali?? N, Simonneau G. The fifth world symposium on pulmonary hypertension. *J Am Coll Cardiol* 2013;62:D1–D3.

12. Humbert M, McLaughlin V V. The 4th World Symposium on Pulmonary Hypertension. *J Am Coll Cardiol* 2009;54:S1–S2.

13. Rosenkranz S. Pulmonary hypertension 2015: current definitions, terminology, and novel treatment options. *Clin Res Cardiol* 2015;104:197–207.

14. Dweik RA, Rounds S, Erzurum SC, Archer S, Fagan K, Hassoun PM, Hill NS, Humbert M, Kawut SM, Krowka M, Michelakis E, Morrell NW, Stenmark K, Tuder RM, Newman J, Bloch K, Gaston B. An official American Thoracic Society statement: Pulmonary hypertension phenotypes. *Am J Respir Crit Care Med* 2014;189:345–355.

15. McLaughlin V V., Davis M, Cornwell W. Pulmonary Arterial Hypertension. *Curr Probl Cardiol* 2011;36:461–517.

16. McGoon MD, Benza RL, Escribano-Subias P, Jiang X, Miller DP, Peacock AJ, Pepke-Zaba J, Pulido T, Rich S, Rosenkranz S, Suissa S, Humbert M. Pulmonary arterial hypertension: Epidemiology and registries. *J Am Coll Cardiol*

2013;62:D51–D59.

17. Stenmark KR, Frid MG, Yeager M, Li M, Riddle S, McKinsey T, El Kasmi KC. Targeting the adventitial microenvironment in pulmonary hypertension: A potential approach to therapy that considers epigenetic change. *Pulm Circ* 2012;2:3–14.

18. Humbert M, Sitbon O, Chaouat A, Bertocchi M, Habib G, Gressin V, Yaici A, Weitzenblum E, Cordier J-F, Chabot F, Dromer C, Pison C, Reynaud-Gaubert M, Haloun A, Laurent M, Hachulla E, Simonneau G. Pulmonary Arterial Hypertension in France. *Am J Respir Crit Care Med* 2006;173:1023–1030.

19. Escribano-Subias P, Blanco I, Lopez-Meseguer M, Lopez-Guarch CJ, Roman A, Morales P, Castillo-Palma MJ, Segovia J, Gomez-Sanchez MA, Barbera JA. Survival in pulmonary hypertension in Spain: insights from the Spanish registry. *Eur Respir J* 2012;40:596–603.

20. Ling Y, Johnson MK, Kiely DG, Condliffe R, Elliot CA, Gibbs JSR, Howard LS, Pepke-Zaba J, Sheares KKK, Corris PA, Fisher AJ, Lordan JL, Gaine S, Coghlan JG, Wort SJ, Gatzoulis MA, Peacock AJ. Changing Demographics, Epidemiology, and Survival of Incident Pulmonary Arterial Hypertension. *Am J Respir Crit Care Med* 2012;186:790–796.

21. Maron BA, Zamanian RT, Waxman AB. *Pulmonary Hypertension: Basic Science to Clinical Medicine*. In: Maron BA, Zamanian RT, Waxman AB, editors. *Springer* Cham: Springer International Publishing; 2016. doi:10.1016/B978-1-4557-2532-8.00014-1.

22. Tuder RM, Cool CD, Geraci MW, Wang J, Abman SH, Wright L, Badesch D, Voelkel NF. Prostacyclin synthase expression is decreased in lungs from patients with severe pulmonary hypertension. *Am J Respir Crit Care Med* 1999;159:1925–1932.

23. Gerber JG, Voelkel N, Nies AS, McMurtry IF, Reeves JT. Moderation of hypoxic vasoconstriction by infused arachidonic acid: role of PGI2. *J Appl Physiol Respir Env Exerc Physiol* 1980;49:107–112.

24. Christman BW, McPherson CD, Newman J, King G, Bernard GR, Groves BM, Loyd JE. An Imbalance between the Excretion of Thromboxane and Prostacyclin Metabolites in Pulmonary Hypertension. *N Engl J Med* 1992;327:70–75.

25. Vincent J a, Ross RD, Kassab J, Hsu JM, Pinsky WW. Relation of elevated plasma endothelin in congenital heart disease to increased pulmonary blood flow. *Am J Cardiol* 1993;71:1204–7.

26. Giaid A, Yanagisawa M, Langleben D, Michel RP, Levy R, Shennib H, Kimura S, Masaki T, Duguid WP, Stewart DJ. Expression of endothelin-1 in the lungs of patients with pulmonary hypertension. *N Engl J Med* 1993;328:1732–9.

27. Giaid A, Saleh D. Reduced expression of endothelial nitric oxide synthase in the lungs of patients with pulmonary hypertension. *N Engl J Med* 1995;333:214–212.

28. McQuillan LP, Leung GK, Marsden PA, Kostyk SK, Kourembanas S. Hypoxia inhibits expression of eNOS via transcriptional and posttranscriptional mechanisms. *Am J Physiol* 1994;267:H1921–H1927.

29. Mason NA, Springall DR, Burke M, Pollock J, Mikhail G, Yacoub MH, Polak JM. High expression of endothelial nitric oxide synthase in plexiform lesions of pulmonary hypertension. *J Pathol* 1998;185:313–318.

30. Marcos E, Adnot S, Pham MH, Nosjean A, Raffestin B, Hamon M, Eddahibi S. Serotonin transporter inhibitors protect against hypoxic pulmonary hypertension. *Am J Respir Crit Care Med* 2003;168:487–493.

31. Eddahibi S, Humbert M, Fadel E, Raffestin B, Darmon M, Capron F, Simonneau G, Dartevelle P, Hamon M, Adnot S. Serotonin transporter overexpression is responsible for pulmonary artery smooth muscle hyperplasia in. *J Clin Invest* 2001;108:1141–1150.

32. Hervé P, Launay JM, Scrobohaci ML, Brenot F, Simonneau G, Petitpretz P, Poubeau P, Cerrina J, Duroux P, Drouet L. Increased plasma serotonin in primary pulmonary hypertension. *Am J Med* 1995;99:249–54.

33. Lee SL, Wang WW, Lanzillo JJ, Fanburg BL. Serotonin produces both hyperplasia and hypertrophy of bovine pulmonary artery smooth muscle cells in culture. *Am J Physiol* 1994;266:L46–52.

34. Humbert M, Morrell NW, Archer SL, Stenmark KR, MacLean MR, Lang IM, Christman BW, Weir EK, Eickelberg O, Voelkel NF, Rabinovitch M. Cellular and molecular pathobiology of pulmonary arterial hypertension. *J Am Coll Cardiol* 2004;43:13S–24S.

35. Price LC, Wort SJ, Perros F, Dorfmuller P, Huertas A, Montani D, Cohen-Kaminsky S, Humbert M. Inflammation in pulmonary arterial hypertension. *Chest*

2012;141:210–221.

36. Cool CD, Kennedy D, Voelkel NF, Tuder RM. Pathogenesis and evolution of plexiform lesions in pulmonary hypertension associated with scleroderma and human immunodeficiency virus infection. *Hum Pathol* 1997;28:434–442.

37. Tuder RM, Groves B, Badesch DB, Voelkel NF. Exuberant endothelial cell growth and elements of inflammation are present in plexiform lesions of pulmonary hypertension. *Am J Pathol* 1994;144:275–85.

38. Hall S, Brogan P, Haworth SG, Klein N. Contribution of inflammation to the pathology of idiopathic pulmonary arterial hypertension in children. *Thorax* 2009;64:778–83.

39. Pinto RFA, Higuchi MDL, Aiello VD. Decreased numbers of T-lymphocytes and predominance of recently recruited macrophages in the walls of peripheral pulmonary arteries from 26 patients with pulmonary hypertension secondary to congenital cardiac shunts. *Cardiovasc Pathol* 2004;13:268–275.

40. Soon E, Holmes AM, Treacy CM, Doughty NJ, Southgate L, MacHado RD, Trembath RC, Jennings S, Barker L, Nicklin P, Walker C, Budd DC, Pepke-Zaba J, Morrell NW. Elevated levels of inflammatory cytokines predict survival in idiopathic and familial pulmonary arterial hypertension. *Circulation* 2010;122:920–927.

41. Sanchez O, Marcos E, Perros F, Fadel E, Tu L, Humbert M, Dartevelle P, Simonneau G, Adnot S, Eddahibi S. Role of endothelium-derived CC chemokine ligand 2 in idiopathic pulmonary arterial hypertension. *Am J Respir Crit Care Med*

2007;176:1041–1047.

42. Burke DL, Frid MG, Kunrath CL, Karoor V, Anwar A, Wagner BD, Strassheim D, Stenmark KR. Sustained hypoxia promotes the development of a pulmonary artery-specific chronic inflammatory microenvironment. *AJP Lung Cell Mol Physiol* 2009;297:L238–L250.

43. Li M, Riddle SR, Frid MG, El Kasmi KC, McKinsey TA, Sokol RJ, Strassheim D, Meyrick B, Yeager ME, Flockton AR, McKeon BA, Lemon DD, Horn TR, Anwar A, Barajas C, Stenmark KR. Emergence of Fibroblasts with a Proinflammatory Epigenetically Altered Phenotype in Severe Hypoxic Pulmonary Hypertension. *J Immunol* 2011;187:2711–2722.

44. Rabinovitch M, Guignabert C, Humbert M, Nicolls MR. Inflammation and Immunity in the Pathogenesis of Pulmonary Arterial Hypertension. *Circ Res* 2014;115:165–175.

45. Cool CD, Stewart JS, Werahera P, Miller GJ, Williams RL, Voelkel NF, Tuder RM. Three-Dimensional Reconstruction of Pulmonary Arteries in Plexiform Pulmonary Hypertension Using Cell-Specific Markers. *Am J Pathol* 1999;155:411–419.

46. Taraseviciene-Stewart L, Kasahara Y, Alger L, Hirth P, Mc Mahon G, Waltenberger J, Voelkel NF, Tuder RM. Inhibition of the VEGF receptor 2 combined with chronic hypoxia causes cell death-dependent pulmonary endothelial cell proliferation and severe pulmonary hypertension. *FASEB J* 2001;15:427–438.

47. Gali?? N, Manes A, Branzi A. The endothelin system in pulmonary arterial hypertension. *Cardiovasc Res* 2004;61:227–237.

48. Davie N, Haleen SJ, Upton PD, Polak JM, Yacoub MH, Morrell NW, Wharton J. ET A and ET B receptors modulate the proliferation of human pulmonary artery smooth muscle cells. *Am J Respir Crit Care Med* 2002;165:398–405.

49. Biasin V, Chwalek K, Wilhelm J, Best J, Marsh LM, Ghanim B, Klepetko W, Fink L, Schermuly RT, Weissmann N, Olschewski A, Kwapiszewska G. Endothelin-1 driven proliferation of pulmonary arterial smooth muscle cells is c-fos dependent. *Int J Biochem Cell Biol* 2014;54:137–148.

50. Kovacs L, Han W, Rafikov R, Bagi Z, Offermanns S, Saido TC, Black SM, Su Y. Activation of Calpain-2 by Mediators in Pulmonary Vascular Remodeling of Pulmonary Arterial Hypertension. *Am J Respir Cell Mol Biol* 2015;2:150806101648009.

51. Ma W, Han W, Greer PA, Tuder RM, Toque HA, Wang KKW, Caldwell RW, Su Y. Calpain mediates pulmonary vascular remodeling in rodent models of pulmonary hypertension, and its inhibition attenuates pathologic features of disease. *J Clin Invest* 2011;121:4548–4566.

52. Evans JDW, Girerd B, Montani D, Wang X-J, Galiè N, Austin ED, Elliott G, Asano K, Grünig E, Yan Y, Jing Z-C, Manes A, Palazzini M, Wheeler LA, Nakayama I, Satoh T, Eichstaedt C, Hinderhofer K, Wolf M, Rosenzweig EB, Chung WK, Soubrier F, Simonneau G, Sitbon O, Gräf S, Kaptoge S, Di Angelantonio E, Humbert M, Morrell NW. BMPR2 mutations and survival in

pulmonary arterial hypertension: an individual participant data meta-analysis. *Lancet Respir Med* 2016;2600:1–9.

53. Teichert-Kuliszewska K, Kutryk MJB, Kuliszewski MA, Karoubi G, Courtman DW, Zucco L, Granton J, Stewart DJ. Bone morphogenetic protein receptor-2 signaling promotes pulmonary arterial endothelial cell survival: Implications for loss-of-function mutations in the pathogenesis of pulmonary hypertension. *Circ Res* 2006;98:209–217.

54. Yang X, Long L, Southwood M, Rudarakanchana N, Upton PD, Jeffery TK, Atkinson C, Chen H, Trembath RC, Morrell NW. Dysfunctional Smad signaling contributes to abnormal smooth muscle cell proliferation in familial pulmonary arterial hypertension. *Circ Res* 2005;96:1053–1063.

55. Austin ED, Loyd JE. The Genetics of Pulmonary Arterial Hypertension. *Circ Res* 2014;115:189–202.

56. Gore B, Izikki M, Mercier O, Dewachter L, Fadel E, Humbert M, Dartevelle P, Simonneau G, Naeije R, Lebrin F, Eddahibi S. Key role of the endothelial TGF-β/ALK1/endoglin signaling pathway in humans and rodents pulmonary hypertension. *PLoS One* 2014;9.:

57. Antigny F, Hautefort A, Meloche J, Belacel-Ouari M, Manoury B, Rucker-Martin C, Péchoux C, Potus F, Nadeau V, Tremblay E, Ruffenach G, Bourgeois A, Dorfmüller P, Breuils-Bonnet S, Fadel E, Ranchoux B, Jourdon P, Girerd B, Montani D, Provencher S, Bonnet S, Simonneau G, Humbert M, Perros F. Potassium-Channel Subfamily K-Member 3 (KCNK3) Contributes to the

Development of Pulmonary Arterial Hypertension. *Circulation* 2016;3:CIRCULATIONAHA.115.020951.

58. Masri FA, Xu W, Comhair SAA, Asosingh K, Koo M, Vasanji A, Drazba J, Anand-Apte B, Erzurum SC. Hyperproliferative apoptosis-resistant endothelial cells in idiopathic pulmonary arterial hypertension. *AJP Lung Cell Mol Physiol* 2007;293:L548–L554.

59. Xu W, Koeck T, Lara AR, Neumann D, DiFilippo FP, Koo M, Janocha AJ, Masri FA, Arroliga AC, Jennings C, Dweik RA, Tuder RM, Stuehr DJ, Erzurum SC. Alterations of cellular bioenergetics in pulmonary artery endothelial cells. *Proc Natl Acad Sci* 2007;104:1342–1347.

60. Lunt SY, Vander Heiden MG. Aerobic glycolysis: meeting the metabolic requirements of cell proliferation. *Annu Rev Cell Dev Biol* 2011;27:441–64.

61. Paulin R, Michelakis ED. The Metabolic Theory of Pulmonary Arterial Hypertension. *Circ Res* 2014;115:148–164.

62. Tomaskova Z, Ondrias K. Mitochondrial chloride channels - What are they for? *FEBS Lett* 2010;584:2085–2092.

63. Elmore S. Apoptosis: a review of programmed cell death. *Toxicol Pathol* 2007;35:495–516.

64. Kondratskyi A, Kondratska K, Skryma R, Prevarskaya N. Ion channels in the regulation of apoptosis. *Biochim Biophys Acta - Biomembr* 2015;1848:2532–2546.

65. Galluzzi L, Blomgren K, Kroemer G. Mitochondrial membrane permeabilization

in neuronal injury. *Nat Rev Neurosci* 2009;10:481–494.

66. Vervliet T, Parys JB, Bultynck G. Bcl-2 proteins and calcium signaling: complexity beneath the surface. *Oncogene* 2016;1–14.doi:10.1038/onc.2016.31.

67. Tajeddine N. How do reactive oxygen species and calcium trigger mitochondrial membrane permeabilization? *Biochim Biophys Acta - Gen Subj* 2016;doi:10.1016/j.bbagen.2016.02.013.

68. Dolado I, Swat A, Ajenjo N, De Vita G, Cuadrado A, Nebreda AR. p38α MAP Kinase as a Sensor of Reactive Oxygen Species in Tumorigenesis. *Cancer Cell* 2007;11:191–205.

69. Lang F, Hoffmann EK. Role of Ion Transport in Control of Apoptotic Cell Death. *Compr Physiol* Hoboken, NJ, USA: John Wiley & Sons, Inc.; 2012. p. 2037–2061.

70. Hajn??czky G, Csord??s G, Das S, Garcia-Perez C, Saotome M, Sinha Roy S, Yi M. Mitochondrial calcium signalling and cell death: Approaches for assessing the role of mitochondrial Ca2+ uptake in apoptosis. *Cell Calcium* 2006;40:553–560.

71. Giorgi C, Baldassari F, Bononi A, Bonora M, De Marchi E, Marchi S, Missiroli S, Patergnani S, Rimessi A, Suski JM, Wieckowski MR, Pinton P. Mitochondrial Ca2+ and apoptosis. *Cell Calcium* 2012;52:36–43.

72. Kroemer G, Galluzzi L, Brenner C. Mitochondrial Membrane Permeabilization in Cell Death. *Physiol Reveiw* 2007;99–163.doi:10.1152/physrev.00013.2006.

73. Pinton P, Giorgi C, Siviero R, Zecchini E, Rizzuto R. Calcium and apoptosis: ER-mitochondria Ca2+ transfer in the control of apoptosis. *Oncogene* 2008;27:6407–

18.

74. Gil-Parrado S, Fern??ndez-Montalv??n A, Assfalg-Machleidt I, Popp O, Bestvater F, Holloschi A, Knoch TA, Auerswald EA, Welsh K, Reed JC, Fritz H, Fuentes-Prior P, Spiess E, Salvesen GS, Machleidt W. Ionomycin-activated calpain triggers apoptosis. A probable role for Bcl-2 family members. *J Biol Chem* 2002;277:27217–27226.

75. Chen M, He H, Zhan S, Krajewski S, Reed JC, Gottlieb RA. Bid is Cleaved by Calpain to an Active Fragment in Vitro and during Myocardial Ischemia/Reperfusion. *J Biol Chem* 2001;276:30724–30728.

76. Wang H-G, Pathan N, Ethell IM, Krajewski S, Yamaguchi Y, Shibasaki F, McKeon F, Bobo T, Franke TF, Reed JC. Ca2+-Induced Apoptosis Through Calcineurin Dephosphorylation of BAD. *Science (80-)* 1999;284:339–343.

77. Rizzuto R, Marchi S, Bonora M, Aguiari P, Bononi A, De Stefani D, Giorgi C, Leo S, Rimessi A, Siviero R, Zecchini E, Pinton P. Ca2+ transfer from the ER to mitochondria: When, how and why. *Biochim Biophys Acta - Bioenerg* 2009;1787:1342–1351.

78. Szlufcik K, Missiaen L, Parys JB, Callewaert G, De Smedt H. Uncoupled IP3 receptor can function as a Ca2+-leak channel: cell biological and pathological consequences. *Biol Cell* 2006;98:1–14.

79. Alzayady KJ, Chandrasekhar R, Yule DI. Fragmented inositol 1,4,5-trisphosphate receptors retain tetrameric architecture and form functional Ca2+ release channels. *J Biol Chem* 2013;288:11122–11134.

80. Zhang L, Barritt GJ. Evidence that TRPM8 Is an Androgen-Dependent Ca2 + Channel Required for the Survival of Prostate Cancer Cells Evidence that TRPM8 Is an Androgen-Dependent Ca 2 ⁒ Channel Required for the Survival of Prostate Cancer Cells. *Cancer Res* 2004;64:8365–8373.

81. Yamamura H, Ugawa S, Ueda T, Morita A, Shimada S. TRPM8 activation suppresses cellular viability in human melanoma. *AJP Cell Physiol* 2008;295:C296–C301.

82. Wang Y, Yang Z, Meng Z, Cao H, Zhu G, Liu T, Wang X. Knockdown of TRPM8 Suppresses Cancer Malignancy and Enhances Epirubicin-induced Apoptosis in Human Osteosarcoma Cells. *Int J Biol Sci* 2014;10:90–102.

83. Amantini C, Ballarini P, Caprodossi S, Nabissi M, Morelli MB, Lucciarini R, Cardarelli MA, Mammana G, Santoni G. Triggering of transient receptor potential vanilloid type 1 (TRPV1) by capsaicin induces Fas/CD95-mediated apoptosis of urothelial cancer cells in an ATM-dependent manner. *Carcinogenesis* 2009;30:1320–1329.

84. Amantini C, Mosca M, Nabissi M, Lucciarini R, Caprodossi S, Arcella A, Giangaspero F, Santoni G. Capsaicin-induced apoptosis of glioma cells is mediated by TRPV1 vanilloid receptor and requires p38 MAPK activation. *J Neurochem* 2007;102:977–990.

85. Pal S, Hartnett KA, Nerbonne JM, Levitan ES, Aizenman E. Mediation of neuronal apoptosis by Kv2.1-encoded potassium channels. *J Neurosci* 2003;23:4798–802.

86. McFerrin MB, Turner KL, Cuddapah VA, Sontheimer H. Differential role of IK and BK potassium channels as mediators of intrinsic and extrinsic apoptotic cell death. *Am J Physiol Cell Physiol* 2012;303:C1070–8.

87. Szabò I, Leanza L, Gulbins E, Zoratti M. Physiology of potassium channels in the inner membrane of mitochondria. *Pflügers Arch - Eur J Physiol* 2012;463:231–246.

88. Okada Y, Shimizu T, Maeno E, Tanabe S, Wang X, Takahashi N. Volume-sensitive Chloride Channels Involved in Apoptotic Volume Decrease and Cell Death. *J Membr Biol* 2006;209:21–29.

89. Rubera I, Duranton C, Melis N, Cougnon M, Mograbi B, Tauc M. Role of CFTR in oxidative stress and suicidal death of renal cells during cisplatin-induced nephrotoxicity. *Cell Death Dis* 2013;4:e817.

90. Barrière H, Poujeol C, Tauc M, Blasi JM, Counillon L, Poujeol P. CFTR modulates programmed cell death by decreasing intracellular pH in Chinese hamster lung fibroblasts. *Am J Physiol Cell Physiol* 2001;281:C810–24.

91. Fernandez-Salas E, Suh KS, Speransky V V, Bowers WL, Levy JM, Adams T, Pathak KR, Edwards LE, Hayes DD, Cheng C, Steven AC, Weinberg WC, Yuspa SH. mtCLIC/CLIC4, an Organellular Chloride Channel Protein, Is Increased by DNA Damage and Participates in the Apoptotic Response to p53. *Mol Cell Biol* 2002;22:3610–3620.

92. Eggermont J. Calcium-activated Chloride Channels: (Un)known, (Un)loved? *Proc Am Thorac Soc* 2004;1:22–27.

93. Nilius B, Droogmans G. Amazing chloride channels: an overview. *Acta Physiol Scand* 2003;177:119–147.

94. Miledi R. A Calcium-Dependent Transient Outward Current in Xenopus laevis Oocytes. *Proc R Soc B Biol Sci* 1982;215:491–497.

95. Bader CR, Bertrand D, Schwartz EA. Voltage-activated and calcium-activated currents studied in solitary rod inner segments from the salamander retina. *J Physiol* 1982;331:253–284.

96. Caputo A, Caci E, Ferrera L, Pedemonte N, Barsanti C, Sondo E, Pfeffer U, Ravazzolo R, Zegarra-Moran O, Galietta LJ. TMEM16A, a membrane protein associated with calcium-dependent chloride channel activity. *Science (80-)* 2008;322:590–594.

97. Yang YD, Cho H, Koo JY, Tak MH, Cho Y, Shim W-S, Park SP, Lee J, Lee B, Kim B-M, Raouf R, Shin YK, Oh U. TMEM16A confers receptor-activated calcium-dependent chloride conductance. *Nat* … 2008;455:1210–1215.

98. Schroeder BC, Cheng T, Jan YN, Jan LY. Expression cloning of TMEM16A as a calcium-activated chloride channel subunit. *Cell* 2008;134:1019–29.

99. Qu Z, Yao W, Yao R, Liu X, Yu K, Hartzell C. The Ca 2+ -activated Cl − channel, ANO1 (TMEM16A), is a double-edged sword in cell proliferation and tumorigenesis. *Cancer Med* 2014;3:453–461.

100. Shi Z-Z, Shang L, Jiang Y-Y, Hao J-J, Zhang Y, Zhang T-T, Lin D-C, Liu S-G, Wang B-S, Gong T, Zhan Q-M, Wang M-R. Consistent and Differential Genetic

Aberrations between Esophageal Dysplasia and Squamous Cell Carcinoma Detected By Array Comparative Genomic Hybridization. *Clin Cancer Res* 2013;19:5867–5878.

101. Duvvuri U, Shiwarski DJ, Xiao D, Bertrand C, Huang X, Edinger RS, Rock JR, Harfe BD, Henson BJ, Kunzelmann K, Schreiber R, Seethala RS, Egloff AM, Chen X, Lui VW, Grandis JR, Gollin SM. TMEM16A induces MAPK and contributes directly to tumorigenesis and cancer progression. *Cancer Res* 2012;72:3270–3281.

102. Britschgi A, Bill A, Brinkhaus H, Rothwell C, Clay I, Duss S, Rebhan M, Raman P, Guy CT, Wetzel K, George E, Popa MO, Lilley S, Choudhury H, Gosling M, Wang L, Fitzgerald S, Borawski J, Baffoe J, Labow M, Gaither LA, Bentires-Alj M. Calcium-activated chloride channel ANO1 promotes breast cancer progression by activating EGFR and CAMK signaling. *Proc Natl Acad Sci U S A* 2013;110:E1026–34.

103. Liu W, Lu M, Liu B, Huang Y, Wang K. Inhibition of Ca2+-activated Cl− channel ANO1/TMEM16A expression suppresses tumor growth and invasiveness in human prostate carcinoma. *Cancer Lett* 2012;326:41–51.

104. Ruiz C, Martins JR, Rudin F, Schneider S, Dietsche T, Fischer CA, Tornillo L, Terracciano LM, Schreiber R, Bubendorf L, Kunzelmann K. Enhanced Expression of ANO1 in Head and Neck Squamous Cell Carcinoma Causes Cell Migration and Correlates with Poor Prognosis. In: Lo AW, editor. *PLoS One* 2012;7:e43265.

105. Ayoub C, Wasylyk C, Li Y, Thomas E, Marisa L, Robé A, Roux M, Abecassis J,

de Reyniès A, Wasylyk B. ANO1 amplification and expression in HNSCC with a high propensity for future distant metastasis and its functions in HNSCC cell lines. *Br J Cancer* 2010;103:715–726.

106. Simon S, Grabellus F, Ferrera L, Galietta L, Schwindenhammer B, Muhlenberg T, Taeger G, Eilers G, Treckmann J, Breitenbuecher F, Schuler M, Taguchi T, Fletcher JA, Bauer S. DOG1 Regulates Growth and IGFBP5 in Gastrointestinal Stromal Tumors. *Cancer Res* 2013;73:3661–3670.

107. Ubby I, Bussani E, Colonna A, Stacul G, Locatelli M, Scudieri P, Galietta L, Pagani F. TMEM16A alternative splicing coordination in breast cancer. *Mol Cancer* 2013;12:75.

108. Davis AJ, Forrest AS, Jepps T a, Valencik ML, Wiwchar M, Singer C a, Sones WR, Greenwood I a, Leblanc N. Expression profile and protein translation of TMEM16A in murine smooth muscle. *AJP Cell Physiol* 2010;299:C948–C959.

109. Thomas-Gatewood C, Neeb ZP, Bulley S, Adebiyi A, Bannister JP, Leo MD, Jaggar JH. TMEM16A channels generate Ca2+-activated Cl- currents in cerebral artery smooth muscle cells. *AJP Hear Circ Physiol* 2011;301:H1819–H1827.

110. Yamamura A, Yamamura H, Zeifman A, Yuan JX-J. Activity of Ca2+-activated Cl-- channels contributes to regulating receptor- and store-operated Ca entry in human pulmonary artery smooth muscle cells. *Pulm Circ* 2011;1:269–79.

111. Sun H, Xia Y, Paudel O, Yang X-R, Sham JSK. Chronic hypoxia-induced upregulation of Ca 2+ -activated Cl − channel in pulmonary arterial myocytes: a mechanism contributing to enhanced vasoreactivity. *J Physiol* 2012;590:3507–

3521.

112. Forrest AS, Joyce TC, Huebner ML, Ayon RJ, Wiwchar M, Joyce J, Freitas N, Davis AJ, Ye L, Duan DD, Singer CA, Valencik ML, Greenwood IA, Leblanc N. Increased TMEM16A-encoded calcium-activated chloride channel activity is associated with pulmonary hypertension. *Am J Physiol Cell Physiol* 2012;303:C1229–43.

113. Wu M-M, Lou J, Song B-L, Gong Y-F, Li Y-C, Yu C-J, Wang Q-S, Ma T-X, Ma K, Hartzell HC, Duan DD, Zhao D, Zhang Z-R. Hypoxia augments the calcium-activated chloride current carried by anoctamin-1 in cardiac vascular endothelial cells of neonatal mice. *Br J Pharmacol* 2014;171:3680–3692.

114. Zhang C-H, Li Y, Zhao W, Lifshitz LM, Li H, Harfe BD, Zhu M-S, ZhuGe R. The Transmembrane Protein 16A Ca 2+ -activated Cl − Channel in Airway Smooth Muscle Contributes to Airway Hyperresponsiveness. *Am J Respir Crit Care Med* 2013;187:374–381.

115. Li H, Yan X, Li R, Zhang A, Niu Z, Cai Z, Duan W, Li X, Zhang H. Increased TMEM16A Involved in Alveolar Fluid Clearance After Lipopolysaccharide Stimulation. *Inflammation* 2016;doi:10.1007/s10753-016-0320-8.

Chapter 2

Expression of Ano1 in Pulmonary Endothelial Cells

Abstract

Rationale: Although CaCC currents have been detected in pulmonary ECs, the presence of CaCC remained unclear due to the lack of any molecular candidates. In 2008 Ano1 was confirmed as a molecular candidate for CaCC. Subsequent studies have shown that Ano1 is present in vascular smooth muscle cells and cardiac vascular endothelial cells. However, the presence of Ano1 in pulmonary ECs was not known. We therefore set out to characterize the expression and localization of Ano1 in pulmonary ECs and determine whether Ano1 expression is altered in PAH, a disease that has hyperproliferative pulmonary ECs.

Methods: Ano1 expression in RLMVEC was confirmed using immunoblot. Mitochondrial localization was evaluated in RLMVECs using confocal microscopy and subcellular fractionation. Ano1 currents were measured in RLMVECs using whole cell patch method. Membrane potential changes in RLMVECs were measured using $DiBAC_4(3)$, a membrane potential sensitive dye, along with Eact, a small molecule activator of Ano1. Expression of Ano1 in HPAECs and isolated ECs from control and PAH patients were evaluated by immunoblot. Ano1 expression in an SUH model of PAH was assessed both by histological staining of frozen lung sections and qPCR of freshly isolated lung ECs.

Results: In RLMVECs, we confirmed Ano1 expression and showed via confocal microscopy that Ano1 colocalized to the mitochondria. Subcellular fractionation of RLMVECs also confirmed Ano1 localization to the mitochondrial and membrane fractions. We also verified plasmalemmal Ano1 activity in RLMVECs by detecting

outward rectifying Ano1 currents. Activation of Ano1 using Eact caused a significant hyperpolarization of cellular membrane potential.

Next, we determined that Ano1 is expressed in commercial HPAECs and isolated ECs from control and IPAH patient lungs. We found that Ano1 expression appeared to be elevated from IPAH-ECs. Ano1 localized to the endothelial cells in normoxic and SUH rats, and was also present in plexiform-like lesions from SUH rats. Quantitatively, we found Ano1 was significantly elevated from freshly isolated SUH ECs compared to normoxic controls.

Conclusion: Ano1 appears to be ubiquitously expressed in pulmonary ECs with Ano1 being expressed in RLMVECs, HPAECs, and isolated ECs from control and IPAH patients. Ano1 currents are present in RLMVECs, with activation by Eact resulting in hyperpolarization of membrane potential. Also, Ano1 not only localizes to the membranous fraction but is also present in mitochondria as well. Ano1 expression is elevated in lung ECs from both IPAH patients and rat SUH model of PAH when compared to respective controls. However, the function of Ano1 in pulmonary ECs and role in PAH remains unclear.

Introduction

Chloride channels such as volume-regulated anion channels (VRAC), CFTR, members of the ClC family, CLIC family, CLCA family, and CaCC have all been demonstrated to be present in the pulmonary endothelium (1). However, the presence of CaCC has long been understudied in the endothelium due to the absence of any cloned channel that fit the biophysical attributes of CaCC (1). It has been suggested that members of the ClC, CLCA, and bestrophin family of channels could be molecular candidates of CaCC. However, their sensitivity to calcium as the gating molecule of CaCC was often beyond the physiological concentrations of $[Ca^{2+}]_i$ and the conductance was not similar to that of CaCC (2) (1).

Following the cloning of Ano1, numerous studies associated Ano1 levels with the proliferation that occurs in several cancer types and cell lines (3–10). Beyond these cancer studies, it is not known whether Ano1 can regulate proliferation in non-malignant cells. Pulmonary expression of Ano1 to date has been confirmed in airway smooth muscle (ASM), in alveolar epithelial cells, and PASMC (11–13).

Physiologically, Ano1 expression and activity have been shown to increase and contribute to airway hyperresponsiveness in a mouse model of asthma (13). Ano1 in the alveolar space has been demonstrated to be protective in an acute lung injury model, whereby LPS increased both Ano1 expression and activity (14). The increase in Ano1 expression and activity in airway epithelial cells assisted in increasing alveolar fluid clearance (14). In monocrotaline and chronic hypoxia rodent models of pulmonary hypertension (PH), it has been shown that Ano1 levels are elevated in PASMCs. In these PH models, Ano1 enhanced contractility of the pulmonary artery (12, 15).

Pulmonary Arterial Hypertension (PAH) is classified as group 1 PH and is a severe disorder characterized by a mean pulmonary artery pressure (mPAP) of 25mmHg or higher (16). Pulmonary vascular remodeling has long been documented to occur in PH; however, what makes PAH more devastating is the severity of remodeling (17). In addition to PASMC proliferation that causes medial hypertrophy, dysregulated EC proliferation is present in PAH as well (18). Uncontrolled EC proliferation results in the formation of occlusive plexiform-lesions to form, which then exacerbates PVR (19).

Although Ano1 has been showed to be expressed in several pulmonary tissue types, it is not known whether Ano1 is expressed in pulmonary ECs. Moreover, some have demonstrated Ano1 levels are increased in rodent models of PH; however, none have determined if Ano1 levels are also elevated in the more proliferative setting of PAH. We hypothesized that Ano1 would express in endothelial cells, and Ano1 levels would increase in settings of PAH. We set out initially to characterize the expression and localization of Ano1 in pulmonary ECs. We then investigated whether Ano1 expression would change in ECs in settings of PAH.

Materials and Methods

Antibodies and Reagents

Antibodies against Ano1, COX IV, and GAPDH were all purchased from Cell Signaling Technologies (Beverly, MA). Antibody against Actin was purchased from Santa Cruz Biotechnologies (Dallas, TX). Antibody against Vinculin was obtained from

Sigma (St. Louis, MO). Alexa Fluor 488 secondary antibody was obtained from Jackson ImmunoResearch Labs (West Grove, PA).

Complete MCDB-131 was purchased from Vec Technologies (Rensselaer, NY) while serum-free MCDB-131 was obtained from Gibco (Grand Island, NY). For human ECs, fibronectin was purchased from EMD Millipore (Billerica, MA). EGM-2 and EBM-2 media were obtained from Lonza (Walkersville, MD).

DC Protein Assay and Clarity ECL were purchased from BioRad (Hercules, CA). MitoTracker Deep Red and Prolong Gold Antifade were both from ThermoFisher Scientific (Agawam, MA). Tissue-Tek OCT was obtained from VWR (Visalia, CA). FOCUS SubCell kit was purchased from G-Biosciences (St. Louis, MO). Dynabead Goat Anti-Mouse were purchased from Life Technologies (Bedford, MA) and antibody against CD-31 from BD Biosciences (Bedford, MA).

RNeasy Mini Kit was purchased from Qiagen (Valencia, CA). SuperScript III SuperMix Kit was from Invitrogen (Bedford, MA). SYBR Green Supermix was from BioRad (Bedford, MA). All qPCR primers were supplied by IDT (Coralville, IA). $DiBAC_4(3)$ was from Life Technologies (Bedford, MA).

All other materials were obtained from Sigma (St. Louis, MO).

Cell Culture

Rat Lung Microvascular Endothelial Cells (RLMVECs) were purchased from Vec Technologies (Rensselaer, NY). For all experiments conducted with RLMVECs, cultureware were coated with 0.2% gelatin for 30 minutes at 37 °C. Media use was reserved to either complete MCDB-131 media or serum reduced MCDB-131, which was

made by combining 1/10 complete MCDB-131 and 9/10 serum-free MCDB-131. Cells were quiesced with reduced-serum for 24 hours. For all experiments, passages were kept between passages 4-7. Human Pulmonary Artery Endothelial Cells (HPAECs) were purchased from Lonza (Walkersville, MD) and were used between passages 4-6.

Serpil Erzurum, MD kindly donated two sets of control and IPAH primary ECs. Isolated ECs from patient lungs have been extensively characterized as previously described (18, 20). In all experiments conducted using control or IPAH cells, cultureware were coated with fibronectin (1µg/cm^2)at 37 °C for 1 hour. Media used with the cells was either complete EGM-2 media or serum-reduced media which was made by combining 1/25 complete EGM-2 media with 24/25 EBM-2 media. Cells were quiesced in serum-reduced conditions overnight.

Immunoblot

Lysates were collected from cells using a modified Radioimmunoprecipitation Assay (RIPA) buffer (50mM HEPES 7.5, 150mM NaCl, 5mM EDTA, 5mM EGTA, 20mM NaF, 20mM $Na_4P_2O_7$, 1% Triton-X, 1mM PMSF, 1mM Na_3VO_4, and 1X phosphatase inhibitor cocktail). Protein concentration was measured using a DC protein assay. Equal amounts of protein were denatured using 4X Laemilli buffer (62.5 mM Tris-HCl pH 6.8, 10% glycerol, 1% LDS, 0.005% Bromophenol blue, and 355mM 2-mercaptoethanol) followed by heat shock for 5 min at 95 °C and loaded onto a 7.5% SDS-PAGE gels for Ano1 and sufficiently resolved. Gels were transferred overnight using transfer buffer (20mM Tris-Base, 150mM Glycine, and 7.5% methanol) at 30mA, then blocked for 1 hour using 5% BSA in TBS 0.1% Tween, and incubated overnight with primary antibody (1:1000) in 5% BSA in TBS 0.1% Tween at 4 °C. Following

primary incubation, blots were washed and incubated with secondary HRP-conjugated (1:5000).Blots were then developed using Clarity ECL and visualized with GE Healthcare ImageQuant. To confirm equal protein loading, blots were stripped (100mM 2-mercaptoethanol, 2% SDS, and 62.5mM Tris-HCl) for 5 minutes at 50 °C and probed for Vinculin. Densitometry was evaluated using ImageJ software (21).

Immunofluorescence and Confocal Microscopy

RLMVECs were plated on gelatin-coated glass coverslips and allowed to proliferate until a confluent monolayer formed. Cells were fixed using 4% paraformaldehyde for 10 minutes, blocked for 1 hour with 10% donkey serum, then incubated with Ano1 antibody in 10% donkey serum for 1 hour using a 1/200 dilution. Cells were then stained with secondary antibody either Alexa Fluor 488 or 594 as designated in 10 % donkey serum using a 1/200 dilution. Coverslips were the mounted onto slides using ProLong Gold Antifade and sealed using nail polish.

For mitochondrial localization, cells were loaded with 250nM MitoTracker Deep Red for 15 minutes before fixation and permeabilized using 0.1% Triton-X/PBS. Cells were then visualized using a laser-scanning Leica SPII confocal microscope with an oil immersion 60X objective. MitoTracker and Alexa 488 were respectively visualized at an excitation/emission of 644/655nm and 488/525nm. Negative controls were cells that were unstained with MitoTracker Deep Red and only secondary Alexa 488.

Subcellular Fractionation

To isolate various compartments of RLMVECs, we utilized a FOCUS SubCell kit. The manufacturer’s protocol was followed, but in brief, 20 million cells were

collected and homogenized using a Dounce homogenizer. Homogenates were centrifuged at 700g for 10 minutes whereby a nuclear pellet was separated from the other soluble fractions. Remaining fractions were then centrifuged at 12,000g for 15 min to obtain a mitochondrial pellet. The remaining cytosolic and membrane fractions were then separated by centrifuging at 100,000g for 60 minutes to obtain a membrane pellet. Each fraction was then quantified for protein, and 50 µg protein was denatured in 4X Laemilli buffer and separated on a 7.5 % SDS-PAGE gel. To assess purity, Cox IV, GAPDH, and VE-Cadherin antibodies were used to evaluate mitochondrial, cytosolic, and membrane fractions, respectively. Immunoblot procedures were followed as described above.

Sugen-Hypoxia

All animal protocols used in this study were approved by the Institutional Animal Use and Care Committee (IACUC, protocol 2014-001) at the Providence Veteran Affairs Medical Center.

Sugen-Hypoxia model is an accepted rodent model of PAH that our lab has previously used (22). In brief, adult male Sprague-Dawley rats 150 g were injected subcutaneously with 20mg/kg of SU5416 in a diluent (0.5% carboxymethylcellulose sodium, 0.9% sodium chloride, 0.4% polysorbate 80, and 0.9% benzyl alcohol). Rats were then placed in a normobaric hypoxia chamber at a FiO_2 of 10% for three weeks and then placed under room air conditions for an additional four weeks. For controls, normoxic rats were injected with equal volume of diluent subcutaneously and placed at room air conditions for seven weeks.

Histology and EC Isolation

At the end of seven weeks, rats were euthanized, and lungs were harvested. For frozen tissue fixation, saline solution was perfused through the pulmonary artery to clear blood and then inflation fixed in 10% formalin for 1 hour. Lungs were then washed with PBS and placed in a 30% sucrose solution until lungs were submerged fully. Tissue was then embedded in Tissue-Tek OCT while frozen on a mixture of dry ice and isopentane then stored at -80 °C until sectioned.

For EC isolations, a modified version of a well-characterized protocol was used (23). Modifications include the use of Dynabeads Goat Anti-Mouse and Mouse Anti-Rat CD-31. Instead of second sorting with ICAM-1, freshly isolated cells were plated onto fibronectin-coated glass coverslips for LDL uptake characterization. The remainder of the cells were spun down and used for qPCR analysis immediately.

qPCR Analysis

Total RNA was obtained from freshly isolated ECs using an RNeasy Mini Kit per manufacturer directions. Total RNA was digested using RNase-free DNase to remove genomic contamination. RNA was quantified using UV spectroscopy, whereby a final amount of 1 µg of RNA was used in a SuperScript III Kit. After obtaining a cDNA library, qPCR was performed using SYBR Green according to the manufacturer's protocol and duplicates for each sample were run together. Ano1 primers were generated with Primer-BLAST using accession number NM_157817234 (NCBI) while 18s rRNA primer was obtained as previously characterized (See Table 1) (24). The thermal cycling setup for qPCR was as follows: a holding stage for 10 minutes at 95 °C, 15 seconds at 95

°C followed by 1 minute at 60 °C for 40 cycles, and finally a melt curve stage for 15 seconds at 95 °C then 1 minute at 60 °C 15 seconds at 95 °C.

Whole Cell Patch Clamp

Whole-cell patch-clamp recordings were performed on RLMVECs plated on 35-mm tissue culture dishes. Recordings were made with an Axopatch 200B amplifier (Axon Instruments). Briefly, pipette solution contained in mM: 130 CsCl, 10 EGTA, 10 HEPES, 1 $MgCl_2$, and a pH of 7.3. Free calcium concentration in pipette solution was calculated using Maxchelator whereby a final free Ca^{2+} concentration of 600nM was used. The extracellular bath solution contained, in mM: 150 NaCl, 10 Mannitol, 1 $CaCl_2$, 10 $MgCl_2$, 10 HEPES, 10 Glucose, and a pH of 7.2. The currents were recorded at room temperature. A ramp protocol ranging from -100 to +100 mV and lasting 250 ms were performed. All data was acquired using Clampex software and analyzed with Clampfit software (Axon Instruments).

DiBAC4(3) Live Cell Fluorescence

For all imaging experiments, RLMVECs were plated onto 0.1% gelatin-coated glass coverslips and allowed to adhere overnight. Cells were then washed twice with Physiological Saline Solution (PSS) (141 mM NaCl, 4.7 mM KCl, 1.8 mM CaCl2, 1.2 mM MgCl2, 10mM HEPES buffer, and 10 mM glucose). To make low chloride PSS, we substituted 141mM NaCl with 121mM Sodium Gluconate ($NaC_6H_{11}O_7$) . In all experiments, exposure times were kept constant.

Changes in resting V_m were performed as previously described (25). Briefly, cells were loaded with 70 nM bis-(1,3-dibutylbarbituric acid)trimethine oxonol

($DiBAC_4(3)$) for 30 minutes at 37 ºC. Once loaded, the glass coverslip was removed and placed in a closed bath imaging chamber and perfused with PSS and $DiBAC_4(3)$ and imaged until a stable baseline was obtained. The cells were imaged at 40X magnification using an excitation wavelength of 405 nm and a bandpass filter for the emission wavelength of 516 nm.

Data Analysis

Either unpaired two-tailed Student's t-test, One, or Two-Way ANOVA was used when indicated to determine significant differences between means. Data is expressed as mean ± standard error of mean (SEM) unless otherwise indicated. For ANOVA analysis, Tukey's post-hoc analysis was used to determine significance. A P-value < 0.05 was considered statistically significant.

Results

Ano1 is Expressed in Pulmonary Endothelial Cells

We assessed Ano1 expression by immunoblot of RLMVECs and HPAECs (Figure 1A), and ECs from isolated control and PAH patient lungs (IPAH-ECs) (Figure 1B). Ano1 is expressed in all pulmonary ECs aforementioned.

Ano1 is Localized to the Membrane and Mitochondrial Fractions

Using immunofluorescence, we assessed endogenous Ano1 expression first in intact non-permeabilized RLMVECs and found Ano1 staining to be lightly stained and punctate (Figure 1C). Next, we assessed permeabilized RLMVECs that were stained for

Ano1 and Mitotracker deep red. Using confocal microscopy, we found that Ano1 co-localized with the mitochondria (Figure 2A). In order to further establish that Ano1 was present in the mitochondria, we performed subcellular fractionation on RLMVECs. Equal amounts (50μg) of subcellular fractions were resolved on an SDS-PAGE gel. Ano1 localized to whole cell homogenates and membranous fractions (Figure 2B). Furthermore, Ano1 appeared to be enriched in the mitochondria while it did not localize to the cytosolic fraction (Figure 2B).

Ano1 Expression in PAH

We utilized a seven-week Sugen-Hypoxia rat model of PAH to assess changes in Ano1 expression. Ano1 expressed in the endothelial monolayer of normoxic controls and SUH rats (Figure 1D). In addition, Ano1 in SUH lung slices stained at the sites of plexiform-like lesions (Figure 1D).

To quantitatively evaluate Ano1 expression, ECs were isolated from seven-week SUH and normoxic controls and Ano1 expression was assessed using qPCR. We found that Ano1 expression was significantly increased (almost two-fold) in ECs isolated from SUH lungs compared to normoxic controls (Figure 1E). Next, we assessed Ano1 expression from ECs isolated from human lungs. Similar to our animal model findings, Ano1 levels from passage 5 IPAH-ECs were elevated when compared to control ECs (Figure 1B). However, by passage 6 there was no notable difference in expression of Ano1 (Figure 1B).

Ano1 is Active in RLMVECs

In order to evaluate whether Ano1 channels were active in RLMVECs, we used whole cell patch clamp on RLMVECs. We detected outward rectifying Ano1 currents in RLMVECs that were inhibited by 10μM T16Ainh-A01, a specific Ano1 inhibitor (Figure 3A).

We then evaluated whether activation of Ano1 could alter resting membrane potential. We utilized a novel small molecular activator of Ano1, Eact, in combination with $DiBAC_4(3)$ and live cell fluorescence microscopy. Decreases in $DiBAC_4(3)$ are indicative of hyperpolarization. DiBAC4(3) changes were measured as previously described (25–27). 10μM of Eact caused a time-dependent decrease in fluorescence in RLMVECs, indicating that opening of Ano1 results in a significant hyperpolarization of membrane potential (Figure 3B).

We utilized low chloride physiological saline solution (30mM Cl^-) and DIDS (chloride channel inhibitor) to confirm that Eact-induced hyperpolarization was mediated by Cl^-. Both low chloride and DIDS attenuated the hyperpolarization induced by Eact (Figure 3B), indicating Eact-induced membrane chloride currents were responsible for cell hyperpolarization

Discussion

While others have reported that Ano1 is expressed in cardiac microvascular ECs, this is the first study that demonstrates Ano1 expression in pulmonary ECs (28). This demonstrates that Ano1 is not only expressed in PASMCs but is also present in pulmonary ECs where it is conducts currents and activation can evoke cell membrane

hyperpolarization (12, 15, 28, 29). Our finding that activation of Ano1 resulted in a hyperpolarization of membrane potential is consistent with the average resting membrane potential of ECs around -26mV (30).

This study is the first to demonstrate that Ano1 is localized to both the membrane and mitochondria as assessed by confocal microscopy and subcellular fractionation. Our subcellular fractionation indicates that Ano1 is significantly enriched in the mitochondrial fraction. This finding is in line with our immunofluorescence staining of Ano1 in RLMVECs; when comparing our staining for Ano1 in intact non-permeabilized and permeabilized RLMVECs immunofluorescence, we note that Ano1 staining is more pronounced in permeabilized cells which colocalized to the mitochondria.

Several groups have documented the presence of several ion channels and transporters in the mitochondria, the presence of a calcium-activated chloride channel is a novel finding (31). A few anion channels are present in the mitochondria including IMAC (Inner Membrane Anion Channel – molecular identity unknown), VRAC (Volume-Regulated Anion Channel – molecular identity unknown), CLIC4 (Chloride Intracellular Channel 4), and CLIC5 (Chloride Intracellular Channel 5) (31–35). Although widely debated, these channels have been suggested to regulate various mitochondrial functions including $\Delta\Psi_m$, ROS, mitochondrial volume, and pH (36–38). Additionally, these channels have been implicated in regulating apoptosis due to their ability to regulate mitochondrial function (31, 39, 40).

Whether Ano1 could alter mitochondrial function is unknown, and is investigated in chapter 3. Depending on where Ano1 localizes (IMM vs OMM) it could regulate several functions including changes in $\Delta\Psi_m$, oxidative phosphorylation, alterations in

mtROS signaling, and regulation of mitochondrial pH and volume. Mitochondrial CLIC4 has been shown to translocate to the mitochondria where it induces p53 dependent apoptosis (31). It is not known whether Ano1 can undergo similar trafficking intracellularly. Hence, further studies are needed to elucidate the localization and trafficking of Ano1 subcellularly. This will be discussed further in chapter 4.

Other groups have shown that in rodent models of PH, Ano1 in PASMC and cardiac vascular ECs is increased (12, 15, 28, 29). Nevertheless, it was unknown whether Ano1 levels would increase in settings of PAH, where the proliferation of pulmonary ECs is enhanced. Our results indicate that Ano1 levels are increased in the SUH model of PAH. In similar fashion, we found that Ano1 expression was elevated in passage 5 IPAH-ECs when compared to control ECs. However, the increase in Ano1 expression was transient and returned to baseline by passage 6. This discordance in expression levels could be due to in-vitro cell culture conditions; the ECs used in culture were not exposed to a pathophysiological environment such as inflammation, aberrant flow, or hypoxic conditions.

This study is the first to demonstrate that Ano1 levels change in ECs in PAH. However, it is unclear how Ano1 expression upregulated in PAH. IL-4 levels have been shown to increase in PAH and SUH model (41, 42). IL-4 has also been shown to increase expression of Ano1 by the transcriptional activator STAT6 (43). It is, therefore, plausible that elevated Ano1 expression is PAH is triggered by increases in IL-4. However, future studies will be needed to determine whether Ano1 expression alone plays a protective or detrimental role in the pathogenesis of PAH. This will be discussed further in chapter 4.

Acknowledgments

Serpil Erzurum, M.D. kindly provided primary human ECs from control and IPAH patients

Alexander Vang, A.B. had initially immunoblotted for Ano1 in RLMVECs and HPAECs

CardioPulmonary COBRE, Julie Newton, and Julie Braza performed EC isolation from normoxic and SUH rats

Richard Clements, Ph.D. for his guidance with mitochondrial isolations

Dmitry Terentyev, Ph.D. for his assistance with confocal microscopy

Anlong Li, M.D./Ph.D for his assistance with qPCR primer design and whole cell patching

Tables and Figures

Table 1: Primer sequences used for qPCR analysis of isolated ECs.

Primer	Forward (5'-3')	Reverse
Ano1	CGGGTCTCACTGATGTGGT	TGACGAGGATACCAAAATCCA
18S	AGCTGGAATTACCGCGGC	CGGCTACCACATCCAAGGAA

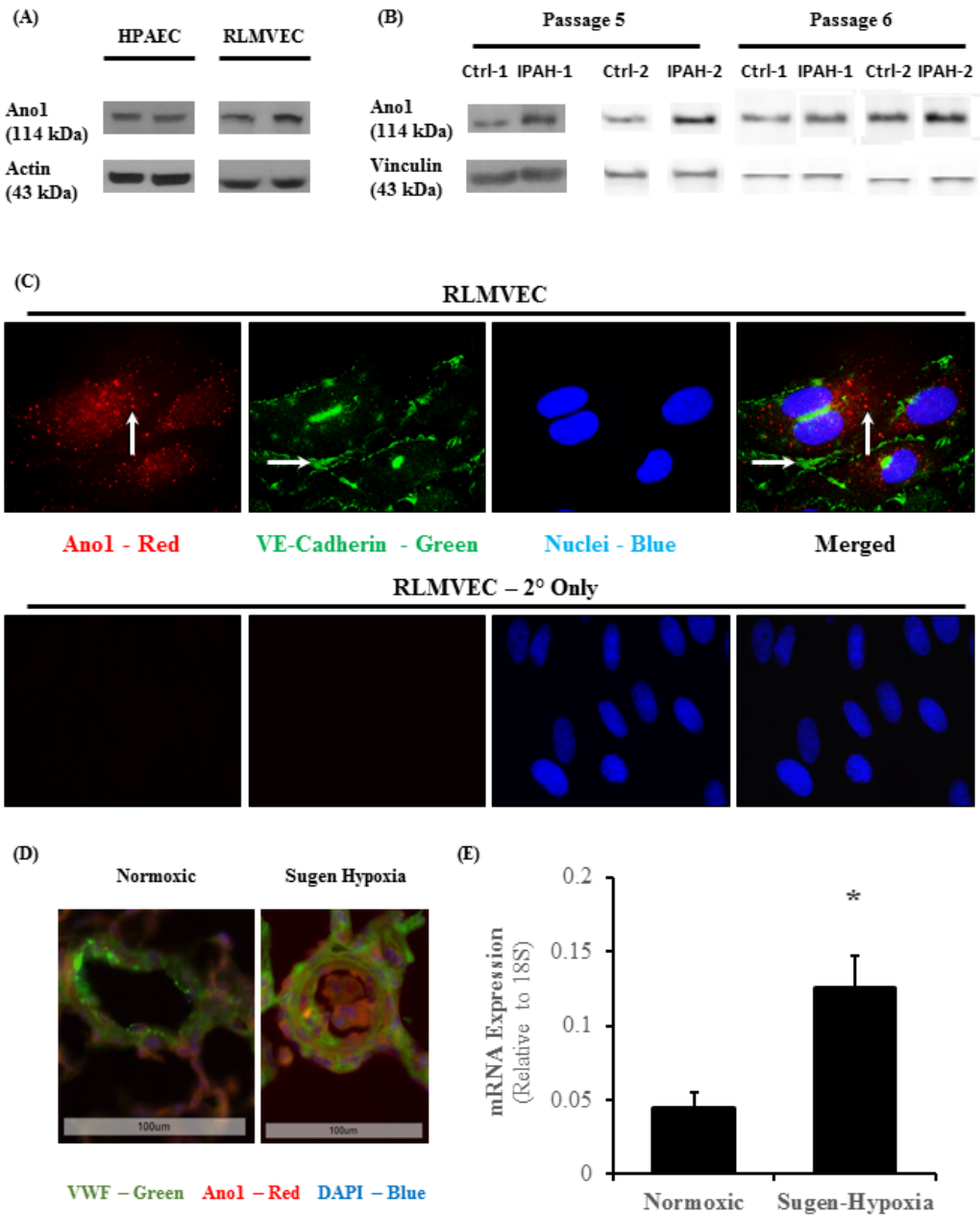

Figure 1: Ano1 expression was evaluated in primary pulmonary endothelial cells. **A)** Ano1 expression was evaluated using immunoblot of HPAECs and RLMVECs lysates, n = 4. **B)** Ano1 expression was assessed from lysates of isolated control and IPAH endothelial cells from human patient lungs. **C)** Endogenous Ano1 localization in non-permeabilized RLMVECs demonstrating punctate (white arrow) Ano1 plasmalemmal localization and VE-Cadherin staining (white arrow) as a marker for endothelial cells. **D)** Ano1 expressed in the pulmonary endothelium and plexiform-like lesions of frozen lung slices from a seven-week Sugen-Hypoxia model of PAH (n = 3). **E)** Ano1 mRNA expression was assessed from freshly isolated ECs using a seven-week Sugen-Hypoxia model and normoxic controls (n = 6, * = $p < 0.05$, compared to control).

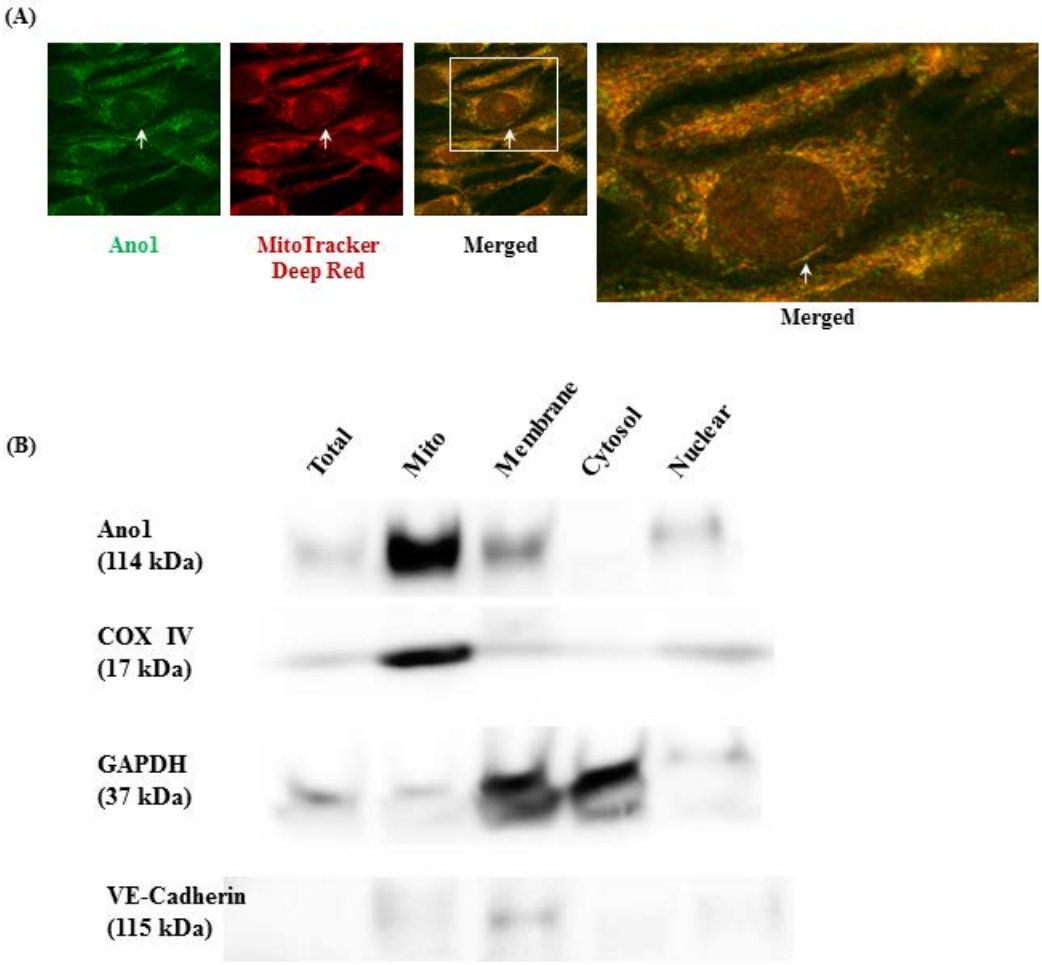

Figure 2: Evaluation of Ano1 localization to the mitochondria of RLMVECs. **A)** Confocal microscopy of permeabilized RLMVECs stained with MitoTracker Deep Red and Ano1 stained using Alexa Fluor 488. Colocalization of staining highlighted with white arrows (n = 3). **B)** Ano1 expression in total homogenate, mitochondrial, membrane, cytosolic, and nuclear fractions was evaluated using subcellular fractionation of RLMVECs (n = 5).

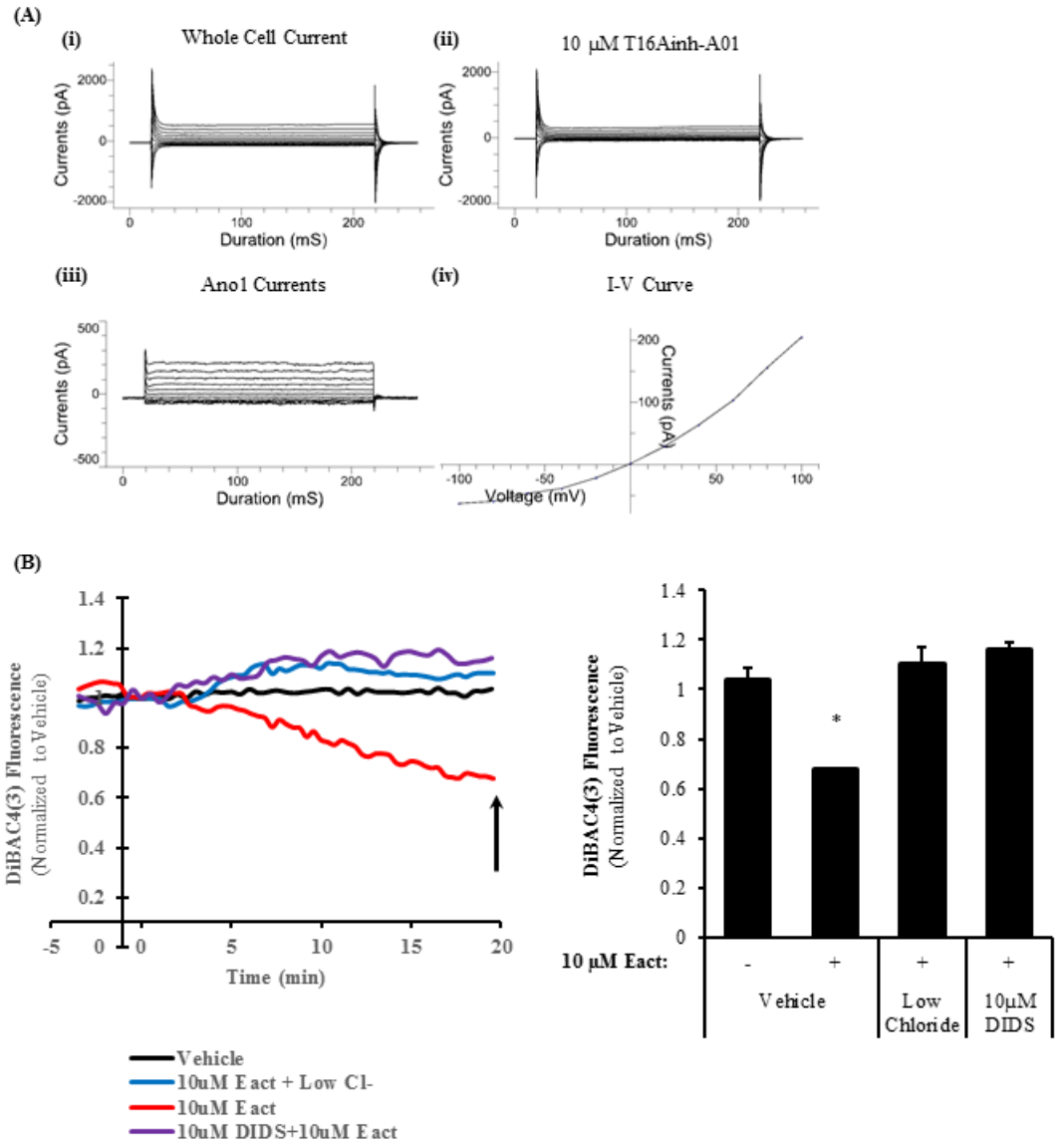

Figure 3: Ano1 is functionally active and conducts current which results in hyperpolarization of resting membrane potential. **A)** Whole cell patch clamp of RLMVECs shows (i) whole cell currents, (ii) whole cell currents in the presence of Ano1 inhibitor T16Ainh-A01 (10µM), (iii) Ano1 currents, and an I-V curve of Ano1 currents **B)** Live cell $DiBAC_4(3)$ fluorescence was measured in a perfusion chamber. RLMVECs were pre-treated with 10µM DIDS, low-chloride PSS (30mM Cl^-), or vehicle then perfused with 10µM Eact and recorded for 20 minutes. DiBAC4(3) fluorescence at the last time point of recording (black arrow) represented in a bar chart (n = 3-5, ANOVA with Tukey Multiple Comparison, * = $p < 0.05$).

References

1. Nilius B, Droogmans GUY. Ion channels and their functional role in vascular endothelium. *Physiol Rev* 2001;81:1415–1459.

2. Matchkov V V. Mechanisms of cellular synchronization in the vascular wall. Mechanisms of vasomotion. *Dan Med Bull* 2010;57:B4191.

3. Duvvuri U, Shiwarski DJ, Xiao D, Bertrand C, Huang X, Edinger RS, Rock JR, Harfe BD, Henson BJ, Kunzelmann K, Schreiber R, Seethala RS, Egloff AM, Chen X, Lui VW, Grandis JR, Gollin SM. TMEM16A induces MAPK and contributes directly to tumorigenesis and cancer progression. *Cancer Res* 2012;72:3270–3281.

4. Qu Z, Yao W, Yao R, Liu X, Yu K, Hartzell C. The Ca 2+ -activated Cl − channel, ANO1 (TMEM16A), is a double-edged sword in cell proliferation and tumorigenesis. *Cancer Med* 2014;3:453–461.

5. Mazzone A, Eisenman ST, Strege PR, Yao Z, Ordog T, Gibbons SJ, Farrugia G. Inhibition of cell proliferation by a selective inhibitor of the Ca2+-activated Cl-channel, Ano1. *Biochem Biophys Res Commun* 2012;427:248–253.

6. Jia L, Liu W, Guan L, Lu M, Wang K. Inhibition of calcium-activated chloride channel ANO1/TMEM16A suppresses tumor growth and invasion in human lung cancer. *PLoS One* 2015;10:1–17.

7. Liu W, Lu M, Liu B, Huang Y, Wang K. Inhibition of Ca2+-activated Cl− channel ANO1/TMEM16A expression suppresses tumor growth and invasiveness in

human prostate carcinoma. *Cancer Lett* 2012;326:41–51.

8. Jacobsen KS, Zeeberg K, Sauter DRP, Poulsen KA, Hoffmann EK, Schwab A. The role of TMEM16A (ANO1) and TMEM16F (ANO6) in cell migration. *Pflugers Arch Eur J Physiol* 2013;465:1753–1762.

9. Ruiz C, Martins JR, Rudin F, Schneider S, Dietsche T, Fischer CA, Tornillo L, Terracciano LM, Schreiber R, Bubendorf L, Kunzelmann K. Enhanced Expression of ANO1 in Head and Neck Squamous Cell Carcinoma Causes Cell Migration and Correlates with Poor Prognosis. In: Lo AW, editor. *PLoS One* 2012;7:e43265.

10. Stanich JE, Gibbons SJ, Eisenman ST, Bardsley MR, Rock JR, Harfe BD, Ordög T, Farrugia G. Ano1 as a regulator of proliferation. *AJP Gastrointest Liver Physiol* 2011;301:G1044–G1051.

11. Bulley S, Neeb ZP, Burris SK, Bannister JP, Thomas-Gatewood CM, Jangsangthong W, Jaggar JH. TMEM16A/ANO1 channels contribute to the myogenic response in cerebral arteries. *Circ Res* 2012;111:1027–1036.

12. Forrest AS, Joyce TC, Huebner ML, Ayon RJ, Wiwchar M, Joyce J, Freitas N, Davis AJ, Ye L, Duan DD, Singer CA, Valencik ML, Greenwood IA, Leblanc N. Increased TMEM16A-encoded calcium-activated chloride channel activity is associated with pulmonary hypertension. *Am J Physiol Cell Physiol* 2012;303:C1229–43.

13. Zhang C-H, Li Y, Zhao W, Lifshitz LM, Li H, Harfe BD, Zhu M-S, ZhuGe R. The Transmembrane Protein 16A Ca 2+ -activated Cl − Channel in Airway Smooth Muscle Contributes to Airway Hyperresponsiveness. *Am J Respir Crit Care Med*

2013;187:374–381.

14. Li H, Yan X, Li R, Zhang A, Niu Z, Cai Z, Duan W, Li X, Zhang H. Increased TMEM16A Involved in Alveolar Fluid Clearance After Lipopolysaccharide Stimulation. *Inflammation* 2016;doi:10.1007/s10753-016-0320-8.

15. Sun H, Xia Y, Paudel O, Yang X-R, Sham JSK. Chronic hypoxia-induced upregulation of Ca 2+ -activated Cl − channel in pulmonary arterial myocytes: a mechanism contributing to enhanced vasoreactivity. *J Physiol* 2012;590:3507–3521.

16. Shah SJ. Pulmonary Hypertension. *JAMA* 2012;308:1366.

17. Paulin R, Michelakis ED. The Metabolic Theory of Pulmonary Arterial Hypertension. *Circ Res* 2014;115:148–164.

18. Masri FA, Xu W, Comhair SAA, Asosingh K, Koo M, Vasanji A, Drazba J, Anand-Apte B, Erzurum SC. Hyperproliferative apoptosis-resistant endothelial cells in idiopathic pulmonary arterial hypertension. *AJP Lung Cell Mol Physiol* 2007;293:L548–L554.

19. Guignabert C, Tu L, Girerd B, Ricard N, Huertas A, Montani D, Humbert M. New Molecular Targets of Pulmonary Vascular Remodeling in Pulmonary Arterial Hypertension. *Chest* 2015;147:529–537.

20. Comhair SAA, Xu W, Mavrakis L, Aldred MA, Asosingh K, Erzurum SC. Human primary lung endothelial cells in culture. *Am J Respir Cell Mol Biol* 2012;46:723–730.

21. Schindelin J, Rueden CT, Hiner MC, Eliceiri KW. The ImageJ ecosystem: An open platform for biomedical image analysis. *Mol Reprod Dev* 2015;in press:DOI: 10.1002/mrd.22489.

22. Casserly B, Mazer JM, Vang A, Harrington EO, Klinger JR, Rounds S, Choudhary G. C-type natriuretic peptide does not attenuate the development of pulmonary hypertension caused by hypoxia and VEGF receptor blockade. *Life Sci* 2011;89:460–466.

23. Lim Y-C, Garcia-Cardena G, Allport JR, Zervoglos M, Connolly AJ, Gimbrone MA, Luscinskas FW. Heterogeneity of Endothelial Cells from Different Organ Sites in T-Cell Subset Recruitment. *Am J Pathol* 2003;162:1591–1601.

24. Lee MY, Garvey SM, Ripley ML, Wamhoff BR. Genome-wide microarray analyses identify the protein C receptor as a novel calcineurin/nuclear factor of activated T cells-dependent gene in vascular smooth muscle cell phenotypic modulation. *Arterioscler Thromb Vasc Biol* 2011;31:2665–2675.

25. Simon A, Harrington EO, Liu GX, Koren G, Choudhary G. Mechanism of C-type natriuretic peptide-induced endothelial cell hyperpolarization. *Am J Physiol Lung Cell Mol Physiol* 2009;296:L248–56.

26. Simon A, Liu GX, Koren G, Choudhary G. cANF causes endothelial cell hyperpolarization by activation of chloride channels. *Peptides* 2009;30:2337–2342.

27. Vang A, Mazer J, Casserly B, Choudhary G. Activation of endothelial BKCa channels causes pulmonary vasodilation. *Vascul Pharmacol* 2010;53:122–129.

28. Wu M-M, Lou J, Song B-L, Gong Y-F, Li Y-C, Yu C-J, Wang Q-S, Ma T-X, Ma K, Hartzell HC, Duan DD, Zhao D, Zhang Z-R. Hypoxia augments the calcium-activated chloride current carried by anoctamin-1 in cardiac vascular endothelial cells of neonatal mice. *Br J Pharmacol* 2014;171:3680–3692.

29. Yamamura A, Yamamura H, Zeifman A, Yuan JX-J. Activity of Ca2+-activated Cl-- channels contributes to regulating receptor- and store-operated Ca entry in human pulmonary artery smooth muscle cells. *Pulm Circ* 2011;1:269–79.

30. Voets T, Droogmans G, Nilius B. Membrane currents and the resting membrane potential in cultured bovine pulmonary artery endothelial cells. *J Physiol* 1996;497:95–107.

31. O'Rourke B. Mitochondrial ion channels. *Annu Rev Physiol* 2007;69:19–49.

32. O'Rourke B, Cortassa S, Aon M a. Mitochondrial ion channels: gatekeepers of life and death. *Physiology (Bethesda)* 2005;20:303–315.

33. Zoratti M, De Marchi U, Gulbins E, Szab?? I. Novel channels of the inner mitochondrial membrane. *Biochim Biophys Acta - Bioenerg* 2009;1787:351–363.

34. Ponnalagu D, Gururaja Rao S, Farber J, Xin W, Hussain AT, Shah K, Tanda S, Berryman M, Edwards JC, Singh H. Molecular identity of cardiac mitochondrial chloride intracellular channel proteins. *Mitochondrion* 2016;27:6–14.

35. Fernandez-Salas E, Suh KS, Speransky V V, Bowers WL, Levy JM, Adams T, Pathak KR, Edwards LE, Hayes DD, Cheng C, Steven AC, Weinberg WC, Yuspa SH. mtCLIC/CLIC4, an Organellular Chloride Channel Protein, Is Increased by

DNA Damage and Participates in the Apoptotic Response to p53. *Mol Cell Biol* 2002;22:3610–3620.

36. Borecký J, Jezek P, Siemen D. 108-pS channel in brown fat mitochondria might Be identical to the inner membrane anion channel. *J Biol Chem* 1997;272:19282–9.

37. Beavis AD. Properties of the inner membrane anion channel in intact mitochondria. *J Bioenerg Biomembr* 1992;24:77–90.

38. Sorgato MC, Keller BU, Stühmer W. Patch-clamping of the inner mitochondrial membrane reveals a voltage-dependent ion channel. *Nature* 1987;330:498–500.

39. Lang F, Hoffmann EK. Role of Ion Transport in Control of Apoptotic Cell Death. *Compr Physiol* Hoboken, NJ, USA: John Wiley & Sons, Inc.; 2012. p. 2037–2061.

40. Madamba SM, Damri KN, Dejean LM, Peixoto PM. Mitochondrial Ion Channels in Cancer Transformation. *Front Oncol* 2015;5:120.

41. Taraseviciene-Stewart L, Nicolls MR, Kraskauskas D, Scerbavicius R, Burns N, Cool C, Wood K, Parr JE, Boackle SA, Voelkel NF. Absence of T Cells Confers Increased Pulmonary Arterial Hypertension and Vascular Remodeling. *Am J Respir Crit Care Med* 2007;175:1280–1289.

42. Price LC, Wort SJ, Perros F, Dorfmüller P, Huertas A, Montani D, Cohen-Kaminsky S, Humbert M. Inflammation in Pulmonary Arterial Hypertension. *Chest* 2012;141:210–221.

43. Mazzone A, Gibbons SJ, Bernard CE, Nowsheen S, Middha S, Almada LL, Ordog

T, Kendrick ML, Reid Lombardo Km, Shen KR, Galietta LJ V, Fernandez-Zapico ME, Farrugia G. Identification and characterization of a novel promoter for the human ANO1 gene regulated by the transcription factor signal transducer and activator of transcription 6 (STAT6). *FASEB J* 2014;1–12.doi:10.1096/fj.14-258541.

Chapter 3

Activation of Ano1 is Associated with Pulmonary Endothelial Cell Apoptosis

Abstract

Rationale: Ano1 can regulate cell proliferation and cell cycle. We have established Ano1 is expressed in pulmonary ECs and is elevated in ECs from IPAH patient lungs (IPAH-ECs) and SUH model. However, the function of Ano1 in regulating the proliferative potential of pulmonary ECs is unknown. Additionally, it is not known whether Ano1 can serve as a target for attenuating PAH EC proliferation.

Methods: Cell counts were used to assess changes in cell number of RLMVECs and IPAH-ECs as indicated. Propidium iodide (PI) staining and analysis were performed to determine RLMVEC cell cycle alterations. Annexin V/PI staining was done to assess changes in RLMVEC death. Caspase-3 activity was measured using a fluorogenic Ac-DEVD-AMC assay using RLMVEC lysates. p38 phosphorylation and Caspase-3 cleavage in RLMVEC, control EC, and IPAH EC lysates were assessed by immunoblot. siRNA transfection was used to knockdown Ano1. JC-1 staining of RLMVECs was used to measure alterations of mitochondrial membrane potential. MitoSOX, a mitochondrial targeted ROS indicator, was used to measure alterations in mtROS. Immunofluorescence staining of treated RLMVECs was utilized to assess AIF nuclear translocation.

Results: Activation of Ano1 resulted in decreased cell number of RLMVECs and also reduced IPAH EC number when compared to control ECs. Activation of Ano1 did not alter cell cycle but resulted in significantly increased Annexin V positive cells. Caspase-3 activity and cleavage were significantly elevated in response to Ano1 activation. Knockdown of Ano1 demonstrated that the apoptotic effects of Eact were mediated via Ano1. Activation of Ano1 also resulted in increasing p38 phosphorylation after 30 minutes, which subsided at 3 hours of treatment. Loss of mitochondrial

membrane potential and an increase in mtROS occurred in response to Ano1 activation. In addition, AIF nuclear translocation increased following Ano1 activation.

Conclusion: Activation of Ano1 in pulmonary ECs results in apoptosis. Apoptosis in response to Ano1 activation is mediated via increases in mtROS, and subsequent p38 activation, which in turn promotes caspase-3 mediated apoptosis. Additionally, activation of Ano1 also results in increasing AIF nuclear translocation which can promote nuclear fragmentation. Finally, we demonstrate that activation of Ano1, which is increased in IPAH-ECs, results in decreasing IPAH EC number when compared to control ECs. This may be mediated in part by an increased susceptibility to Ano1 activation, which induces selective increases in caspase-3 cleavage in IPAH-ECs when compared to control ECs.

Introduction

Ano1 is linked with increased proliferation, migration, invasiveness, and metastasis associated with cancer (1–3). Clinically, increased Ano1 expression in oral or head and neck squamous cell, and breast cancer correlates with poor prognosis (4). Mechanistically, increased Ano1 expression contributes to increased cell proliferation by increasing Erk1/2 phosphorylation, Akt phosphorylation, activation of EGFR, and activation of CAMK signaling (5, 6). Inhibition of Ano1, either via silencing of Ano1 or pharmacological inhibition, reversed proliferation and tumorigenic phenotypes associated with several cancer types (1, 2, 5, 7, 8).

Ano1's functional role in the vasculature has been mostly studied in vascular smooth muscle cells (VSMCs). Increased Ano1 expression and activity in VSMCs promotes vasoconstriction of several vascular beds (9–15). The mechanism by which Ano1 regulates the vasoreactivity of VSMCs is primarily due to membrane depolarization (V_m) via Cl^- efflux. V_m depolarization of VSMCs results in an increase in $[Ca^{2+}]_i$ via voltage-dependent Ca^{2+} channels resulting in increased vasoconstriction (9–15).

In contrast with Ano1's association with proliferation in cancer studies, conflicting evidence has been found for Ano1-induced proliferation in VSMC. One study has shown that angiotensin-II (Ang-II) mediated vascular remodeling occurs by decreasing Ano1 expression (16). Decreased Ano1 expression in VSMC resulted in increased cell proliferation due to reduced cell cycle arrest (16). Conversely, Ano1 overexpression caused restoration of cell cycle checkpoints resulting in decreased cell proliferation (16).

A subsequent study demonstrated that Ang-II decreased Ano1 expression by disrupting a positive feedback loop between myocardin, a transcriptional activator, and Ano1 (17). This disruption occurred due to Ang-II mediated increases in KLF5, which disrupted the synergistic loop between Ano1 and myocardin (17). This evidence suggests that Ano1 does not necessarily increase cell proliferation in all settings and cell-types by upregulation of proliferative pathways (e.g. Activation of EGFR or proliferative MAPK pathways). Instead, Ano1 could modulate proliferation by altering cell cycle checkpoints, and thus controlling overall cell number.

Vascular remodeling of the pulmonary bed in PAH has been extensively documented and discussed in Chapter 1. Briefly, hyperproliferation of apoptosis resistant ECs plays a significant role in the pathogenesis of PAH. The proliferation of the ECs in PAH ultimately leads to the formation of occlusive plexiform lesions. Addressing this vascular remodeling is necessary, and reversal of dysregulated EC proliferation would be advantageous in PAH.

It is evident that Ano1 can contribute to increased proliferation in several cancers and cell lines. However, the role of Ano1 in regulating cell proliferation, cell cycle, and apoptosis in pulmonary endothelial cells is unknown. We hypothesized that altering Ano1 activity would alter the proliferative potential of pulmonary ECs. We, therefore, set out to investigate whether Ano1 affects pulmonary EC proliferation and if Ano1 could serve as a target in aberrant and proliferative IPAH-ECs.

Materials and Methods

Antibodies and Materials

Antibodies against phosphorylated p38 (T^{180}/Y^{182}), total p38, cleaved caspase-3, caspase-3, and AIF were purchased from Cell Signaling Technologies (Beverly, MA). Antibodies against Actin and all secondary HRP-conjugated antibodies were obtained from Santa Cruz Biotechnologies (Dallas, TX). Antibody against Vinculin was obtained from Sigma (St. Louis, MO). Fluorescent-conjugated secondary antibodies were from Jackson ImmunoResearch Labs (West Grove, PA)

Tris-HCl and glycine were from BioRad (Hercules, CA). Annexin V/PI kit, JC-1, and MitoSOX were all obtained from Life Technologies (Bedford, MA). FITC-conjugated Ano1 siRNA was purchased from GE Dharmacon (Lafayette, CO) and FITC-conjugated scrambled siRNA was purchased from Santa Cruz Biotechnologies (Dallas, TX). Lipofectamine 3000 was obtained from ThermoFisher Scientific (Agawam, MA). Accutase and all other reagents were purchased from Sigma (St. Louis, MO).

Cell Count

For all cell counts, 6-well plates were coated appropriately and then seeded at a cell density of $6x10^4$ cells/well and allowed to adhere overnight. Cells were then quiesced using serum-reduced media for either 24 hours (RLMVECs) or 18 hours (human IPAH cells). Cells were then treated as indicated for 24 hours before trypsinization and counted with a hemocytometer. Cell counts for human ECs isolated from PAH lungs (IPAH-ECs) and Ano1 knockdown were conducted in a blinded fashion and using a BioRad T20 automated cell counter.

Annexin V/Propidium Iodide Staining and Cell Cycle Analysis

RLMVECs were seeded subconfluently and allowed to grow for 24 hours. The cells were then quiesced using serum-reduced media for 24 hours and then treated as indicated. Cells were gently removed using Accutase per manufacturer's recommendation, collected, and washed with PBS once. Using an Annexin V/Dead Cell kit, cells were stained as described by the manufacturer before analysis using flow cytometry. For all experiments, the same forward and side scatter gate was used.

Caspase-3 Activity

RLMVECs were seeded subconfluently in 10 cm dishes ($4x10^5$ cells/dish) and allowed to adhere overnight, then quiesced with reduced serum media for 24 hours. Cells were then treated as indicated. For positive control, cells were heat shocked at 45 °C for 15 minutes before returning to 37 °C for another 15 minutes. Lysates were collected in a caspase-3 lysis buffer (10mM HEPES pH 7.5, 40mM 40mM β-glycerophosphate, 50mM NaCl, 2mM $MgCl_2$, 5mM EGTA, and pH adjusted to 7.5), then lysed using 3 freeze/thaw cycles before centrifuging at 15,000g for 10 minutes at 4 °C. 50µg protein per samples was added to a reaction buffer (40mM HEPES pH 7.5, 20% glycerol, and 4mM DTT) with a final concentration of 50µM Ac-DEVD-AMC (BD Pharmigen, Bedford, MA). Lysates were then incubated at 37 °C for 1 to allow cleavage of Ac-DEVD-AMC. To set up a standard curve, serial dilutions of AMC were setup (14.02, 7.01, 4.38, 2.8, 1.4, 0.7, 0.35, and 0 µg/ml) and added to the plate for the last 5 minutes of incubation at 37 °C to allow for equilibration. All reaction volumes and standard curve volumes were set to 100µl.

Immunoblot

Lysates were collected from cells using a modified radioimmunoprecipitation (RIPA) buffer (50mM HEPES 7.5, 150mM NaCl, 5mM EDTA, 5mM EGTA, 20mM NaF, 20mM $Na_4P_2O_7$, 1% Triton-X, 1mM PMSF, 1mM Na_3VO_4, and 1X phosphatase inhibitor cocktail). Protein was measured using a DC protein assay (BioRad, Hercules, CA) and equal amount of protein was denatured using 4X Laemilli buffer (62.5 mM Tris-HCl pH 6.8, 10% glycerol, 1% LDS, 0.005% Bromophenol blue, and 355mM 2-mercaptoethanol) followed by heat shock for 5 min at 95 °C. Samples were then loaded onto SDS-PAGE gels (10% for p38 blots and 15% for caspase-3 blots) and sufficiently resolved. Gels were transferred overnight using transfer buffer (20mM Tris-Base, 150mM Glycine, and 7.5% methanol) at 30mA, then blocked for 1 hour using 5% BSA in TBS 0.1% Tween and incubated overnight with primary in 5% BSA in TBS 0.1% Tween at 4 °C. Following primary incubation, blots were washed and incubated with HRP-conjugated secondary antibodies (Santa Cruz Biotechnology, Dallas, TX) and developed using Clarity ECL (BioRad, Hercules, CA) and visualized using GE Healthcare. To confirm equal protein loading, blots were stripped (100mM 2-mercaptoethanol, 2% SDS, and 62.5mM Tris-HCl) for 5 minutes at 50 °C and probed for Vinculin. Densitometry was evaluated using ImageJ software (18).

Ano1 Knockdown

For all knockdown experiments, RLMVECs were used at passages P2-4. $2.5x10^5$ RLMVECs/well were seeded and allowed to grow overnight in complete MCDB-131 media. Transfection was carried out the following day per manufacturer's description. siRNA final concentrations were 100nM for both Ano1 and scrambled. About 50%

knockdown efficiency was attained 72 hours' post-transfection as evaluated by immunoblot.

JC-1 and MitoSOX Fluorescence

$1X10^4$ RLMVECs/well were seeded in a black clear-bottomed 96 well plate and allowed to adhere overnight. The following day, cells were treated for 20 minutes and 30 minutes as indicated for JC-1 and MitoSOX staining, respectively. For JC-1 staining, cells were washed twice with PBS and then loaded with 10μM JC-1 in warm PSS for 10 minutes at 37 °C. For MitoSOX staining, cells were washed twice with PBS and then stained with 5μM MitoSOX in warm PSS for 10 minutes at 37 °C. Fluorescence was then measured using a plate reader. For JC-1 staining an Ex/Em of 485/25nm and 528/20nm was used for green JC-1 monomer along with an Ex/Em of 535/25 and 590/35nm for red JC-1 aggregates was used. For MitoSOX staining, an excitation filter of 530/25nm and an emission filter of 590/35nm was used.

Immunofluorescence

RLMVECs were plated onto glass coverslips and allowed to adhere overnight, quiesced for 24 hours, then treated as indicated for 24 hours. Cells were then washed with PBS, fixed with 4% paraformaldehyde for 10 minutes, then blocked with 5% donkey serum for 1 hour. Coverslips were then incubated against AIF (1/500) in 5% donkey serum for 1 hour, washed with PBS, and then incubated with Alexa Fluor 594 conjugated secondary antibody. Coverslips mounted using Prolong Gold DAPI Antifade mountant and sealed with nail polish. Negative controls were slides incubated without primary antibody. Coverslips were visualized using fluorescence microscopy.

Data Analysis

Either unpaired two-tailed Student's t-test, One, or Two-Way ANOVA was used when indicated to determine significant differences between means. Data is expressed as mean ± standard error of mean (SEM) unless otherwise indicated. For ANOVA analysis, Tukey's post-hoc analysis was used to determine significance. A P-value < 0.05 was considered statistically significant.

Results

Ano1 Causes Apoptosis of RLMVECs

Treatment of RLMVECs with 10μM Eact for 24 hours led to a significant decrease in cell number (Figure 1A) that was attenuated in presence of chloride channel inhibitor, DIDS (10μM) (Figure 1A).

A decrease in cell number can be mediated via increased proliferation or cell death. Consequently, we measured changes in cell cycle after 24 hours of treatment with Eact using Propidium Iodide (PI) and flow cytometry. Activation of Ano1 did not result in any changes in the cell cycle (Figure 1B).

We used Annexin V/PI staining in conjugation with flow cytometry on RLMVECs that were treated for 24 hours. Annexin V moves to the cell exterior when cells undergo cell death while PI intercalates into the DNA indicative of cell membrane rupture that occurs in later stages of cell death. Ano1 activation caused a significant

increase in the number of cells with Annexin V fluorescence, indicating that Ano1 activation increased cell death of RLMVECs after 24 hours of treatment (Figure 2A).

We confirmed that Ano1 activation resulted in apoptosis mediated by caspase-3. We utilized a caspase-3 activity assay and immunoblot to determine caspase-3 cleavage. Eact treatment for 24 hours increased both caspase-3 activity (Figure 2B) and caspase-3 cleavage as visualized by the elevations of the 17 and 19 kDa band (Figure 2C).

Eact Mediates RLMVEC Apoptosis via Ano1

In order to confirm that Ano-1 mediated the effects of Eact, molecular suppression of Ano1 expression was performed using siRNA. RLMVECs transfected with Ano1 specific siRNA resulted in a significant reduction (~50%) in Ano1 expression compared to cells transfected with scrambled siRNA (Figure 3A). We next assessed whether knockdown of Ano1 attenuated Eact-mediated increases in caspase-3 cleavage. 24 hours of treatment with Eact caused a significant increase in caspase-3 cleavage, which was attenuated in Ano1 knockdown cells (Figure 3B). Similarly, knockdown of Ano1 attenuated the Eact-mediated decrease in cell number (Figure 3C). Notably, when comparing cell numbers between scrambled and Ano1 siRNA transfections, we did not observe any significant change in cell number (Figure 3C).

Ano1 Activation Increases p38 MAPK Phosphorylation

p38 is an important regulator of apoptosis. In order to determine whether Ano1 activation resulted in caspase-3 cleavage via p38 activation, we treated cells with Eact in presence or absence of 100nM SB203580, a specific and well-characterized p38

inhibitor. Inhibition of p38 activation attenuated the Eact-mediated decrease in cell number (Figure 4A).

Next, we measured changes in p38 phosphorylation (Thr180/Tyr182) in response to Ano1 activation. Eact caused a significant increase in p38 phosphorylation at 30-minutes which subsided after 3 hours (Figure 4B). Since p38 is activated in response to upstream increases in ROS, we pretreated cells with 1μM MitoTEMPO, a mitochondrial targeted antioxidant, prior to Ano1 activation. MitoTEMPO blocked Eact-induced increases in p38 (Figure 4C). Moreover, pretreatment with the chloride channel inhibitor, DIDS, also attenuated Eact-induced p38 phosphorylation (Figure 4C).

Ano1 Activation Results in Changes in Mitochondrial Function

In the prior chapter, we demonstrated that Ano1 localized to the mitochondria. Since Ano1 activation resulted in increased mtROS-dependent p38 activation, we assessed whether Ano1 activation elicited changes in ΔΨm and mtROS levels.

JC-1 fluoresces red when aggregates form in the mitochondria due to high ΔΨm, while in its monomeric form in the cytosol it fluoresces green. Data was normalized as a ratio of red/green fluorescence, and the loss of ΔΨm (i.e. depolarization) would result in decreasing the ratio of red/green. Eact treatment resulted in a significant loss of ΔΨm as measured using JC-1 (Figure 5A). Furthermore, DIDS attenuated Eact-induced changes in ΔΨm (Figure 5A).

Ano1 activation also increased mtROS as assayed using MitoSOX, a targeted mitochondrial dye that measures mitochondrial superoxide levels (Figure 5B).

Pretreatment with DIDS and MitoTEMPO attenuated the significant increase in MitoSOX (Figure 5B).

Apoptotic Inducing Factor (AIF), which is released from the mitochondria in during apoptotic cell death was qualitatively assessed using immunofluorescence. RLMVECs treated for 24 hours with or without Eact. Increased nuclear localization of AIF occurred in RLMVECs treated with Eact when compared to vehicle treated cells (Figure 5C).

Ano1 Activation Differentially Induces Apoptosis of ECs from IPAH Patients

Hyperproliferation of ECs isolated from PAH patients (IPAH-ECs) plays a major role in the pathogenesis of PAH. In the previous chapter, we demonstrated that Ano1 expression increased in settings of PAH. We sought to determine whether activation of Ano1 which caused apoptosis of RLMVEC would also induce apoptosis of IPAH-ECs. Control ECs from donor lungs not used and IPAH-ECs were provided by Serpil Erzurum, M.D. and characterized as previously described (19). In brief, ECs were isolated from main and branching pulmonary arteries, and purity was confirmed using VWF staining, positive staining of H. pomatia (pulmonary artery EC lectin), and absence of G. simplicifolia staining (microvascular EC lectin).

IPAH and control patient ECs were seeded, quiesced, and then treated in reduced serum conditions. At baseline, IPAH-ECs were proliferating at a faster rate than control ECs (Figure 6A). 10μM Eact markedly reduced IPAH EC proliferation, while the effect on control EC proliferation was minimal (Figure 6A). Additionally, chloride channel

inhibition using DIDS did not alter cell counts of IPAH-ECs at baseline, but attenuated Eact-induced decrease in cell number (Figure 6A).

In order to confirm that Eact initiated apoptosis in IPAH EC's, we examined caspase-3 cleavage. Similar to RLMVEC, Ano1 activation also increased in IPAH EC caspase-3 cleavage when compared to Eact-treated control ECs (Figure 6B).

Discussion

Collectively, our data demonstrates that activation of Ano1 causes increased caspase-3 mediated apoptosis. This is mediated by increases in mtROS resulting in increased p38 phosphorylation. p38, a stress response MAPK, has been associated with caspase-3 mediated apoptosis in previous studies, including RLMVECs (20). p38 activity was required to induce apoptosis as inhibition of p38 activity by SB203580 resulted in attenuation of Eact-mediated decrease in cell number. Activation of Ano1 reduced cell number and increased caspase-3 cleavage in IPAH-ECs when compared to control ECs. Additionally, inhibition of Ano1 using DIDS in IPAH-ECs attenuated Eact-induced decrease in cell number, but DIDS alone did not reduce cell number suggesting increased Ano1 expression was not contributing to proliferation.

Prior studies have consistently linked upregulated Ano1 expression and augmented currents with proliferation (5, 21, 22). However, when considering the majority of studies that associate Ano1 with increased proliferation are cancer studies, it is plausible that perhaps Ano1 in non-malignant cells has different effects. Only one

group to date has demonstrated that increased expression of Ano1 in VSMCs resulted in decreased cell proliferation by promoting cell cycle arrest (16, 17).

Here, we show that activation of Ano1 associated with increased apoptosis and that pharmacological activation of Ano1 is capable of reducing hyperproliferative IPAH-ECs. We believe that elevated Ano1 expression does not contribute to the hyperproliferation of ECs. Inhibition of Ano1 attenuates Eact-mediated decrease in EC number. Hence, our data suggests that while Ano1 expression is increased in settings of hyperproliferative ECs, it is likely not associated with increased activity. However, activating Ano1 in these settings with a chemical agonist results in apoptosis of these cells.

How Ano1 activation selectively decreased cell number and increased caspase-3 cleavage of IPAH-ECs when compared to control ECs was not delineated in this study. However, it is possible that elevated Ano1 expression primes IPAH-ECs to undergo Eact-mediated apoptosis. This will be further addressed in chapter 4.

Others have documented that Ano1 knockdown in cancerous cell lines and tumor xenografts decreased proliferation (23). In our experiments, we do not observe any significant changes in cell number between cells transfected with scrambled and Ano1 specific siRNA. Thus, the absence of cell number alterations is in contrast with cancer studies, and Ano1 in RLMVECs under basal conditions does not promote increased proliferation.

Endothelial cell death is known to respond to apoptotic triggers by activation of p38 MAPK, which in turn is capable of inducing caspase-3 mediated apoptosis (20, 24–26). In this study, we demonstrate that activation of Ano1 can result in p38-dependent apoptosis, which is mediated by increases in upstream mtROS. We also show that MitoTEMPO attenuated Eact-mediated decreases in IPAH cell number. This indicates that like RLMVECs, Ano1 activation in IPAH-ECs increases mtROS upstream of p38 and is required for apoptosis.

The existence of mitochondrial chloride ion channels has been widely debated. Mitochondrial CLIC4 and CLIC5 have been suggested to localize to the mitochondria (27). We demonstrated in the previous chapter that Ano1 localized to the mitochondria. Here we exhibit that activation of Ano1 associated with the intrinsic apoptosis pathway.

While our data indicates activation of Ano1 is sufficient to induce apoptosis, the exact mechanism linking elevated mitochondrial chloride, increased ROS, and the loss of $\Delta\Psi m$ is unclear. Drawing similarities from CLIC4, it has been shown that increased CLIC4 expression resulted in p53-dependent apoptosis and loss of $\Delta\Psi m$ (28). However, still the mechanism by which CLIC4 alters mitochondrial function remained unclear. Indeed, mitochondrial chloride channels and their role in the induction of apoptosis remains understudied. This will be discussed in chapter 4.

Acknowledgments

Alexander Vang, A.B. for assisting in blinding cell count experiments

Anlong Li, Ph.D. for performing the whole cell patch clamp

CardioPulmonary COBRE for providing me access to the flow cytometry equipment

N. Richard Kue, B.S. for assisting with the immunofluorescence

Tables and Figures

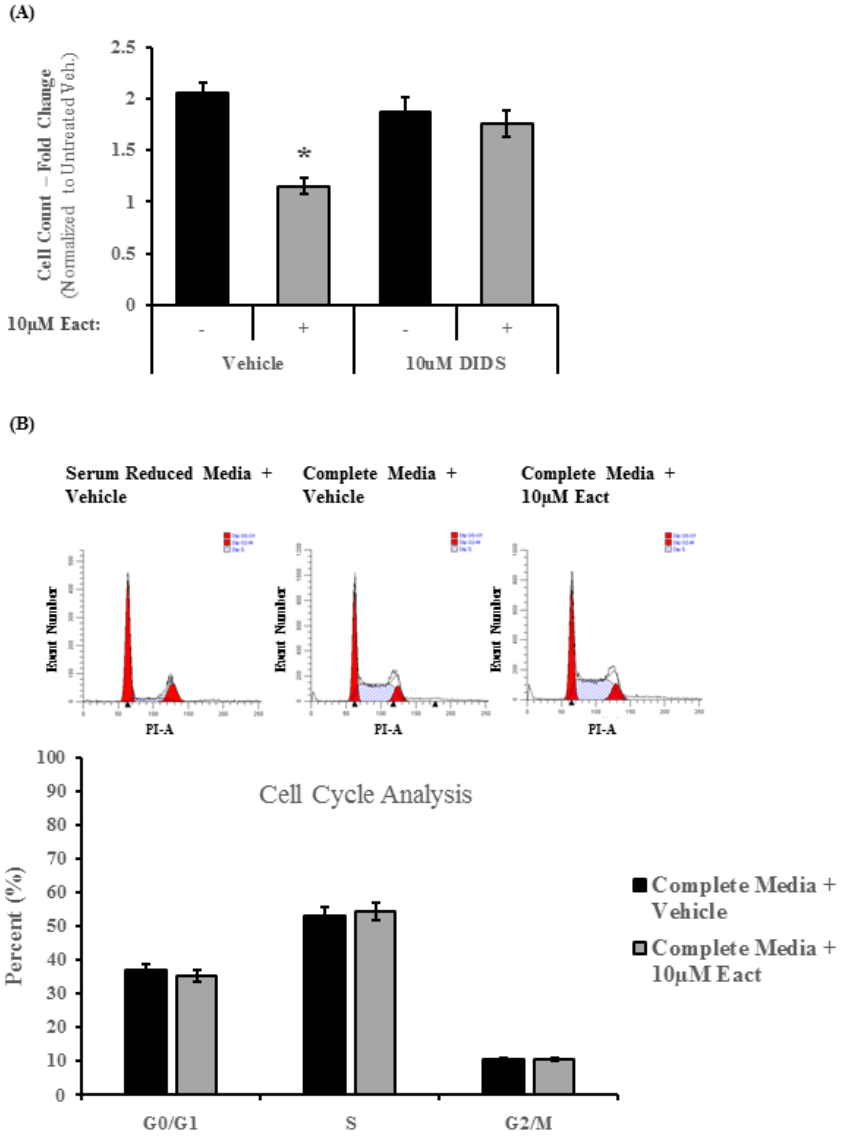

Figure 1: Activation of Ano1 results in decreased cell number, however no alterations in cell cycle occur. **A)** RLMVECs were seeded subconfluently and allowed to adhere before quiescing for 24 hours. Following quiescing, cells were pre-treated with 10μM DIDS or vehicle then treated for 24 hours with 10μM Eact or vehicle after which cell number was assessed using a haemocytometer (n = 4, ANOVA with Tukey Multiple Comparison, $p < 0.05$ vs. untreated control). **B)** RLMVECs were seeded subconfluently and allowed to adhere before quiescing for 24 hours. Following quiescing, cells were treated with 10μM Eact for 24 hours or vehicle. Cells were then fixed and stained with 50μg/ml Propidium Iodide in the presence of RNase A. Cell cycle analysis was performed using ModFit LT (n = 3).

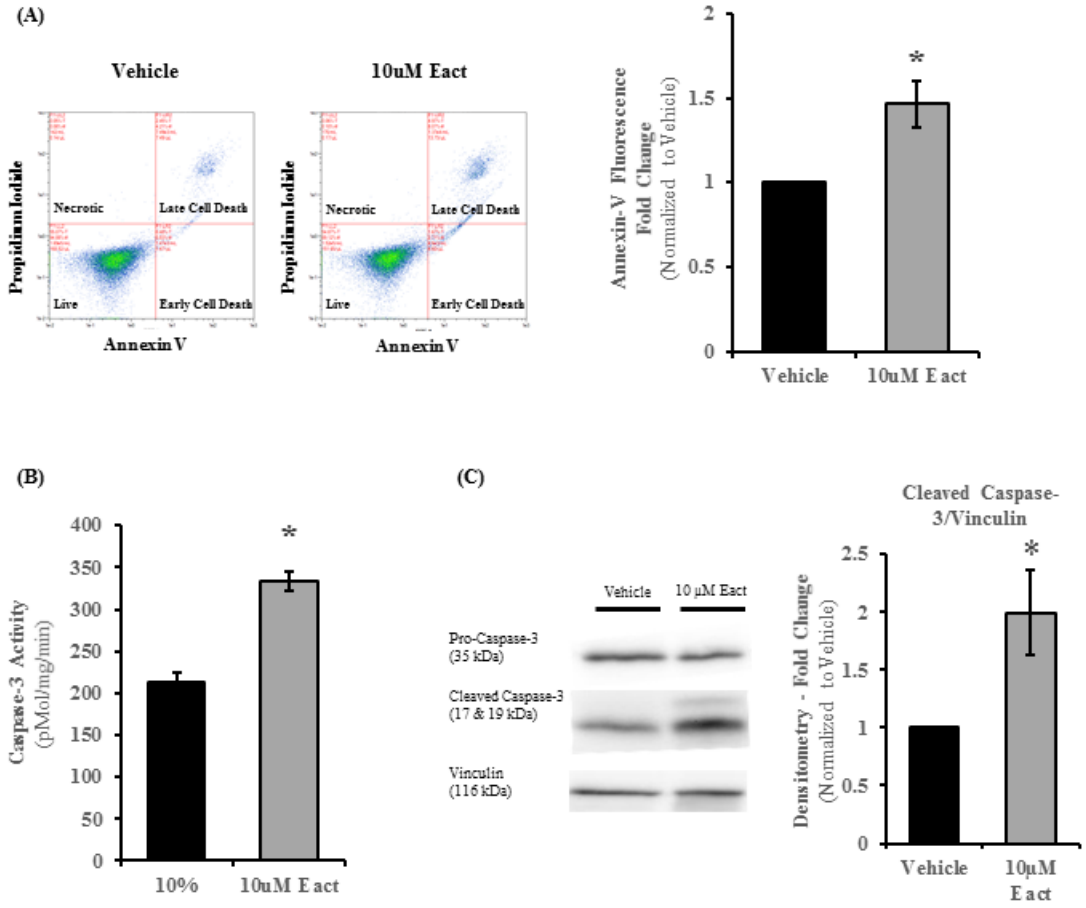

Figure 2: Activation of Ano1 induces apoptosis in RLMVECs. **A)** RLMVECs were seeded subconfluently and allowed to adhere before quiescing for 24 hours. Following quiescing, cells were treated with 10µM Eact or vehicle for 24 hours. Annexin-V/PI fluorescence was then evaluated using flow cytometry and Annexin-V fluorescence was quantified ($n = 6$, $p < 0.05$). **B)** Caspase-3 activity from RLMVECs treated with 10µM Eact or vehicle was measured using a Ac-DEVD-AMC fluorogenic assay ($n = 5$, $p < 0.05$). **C)** Immunoblot of cleaved caspase-3 from RLMVECs treated with 10µM Eact or vehicle for 24 hours ($n = 5$, $p < 0.05$).

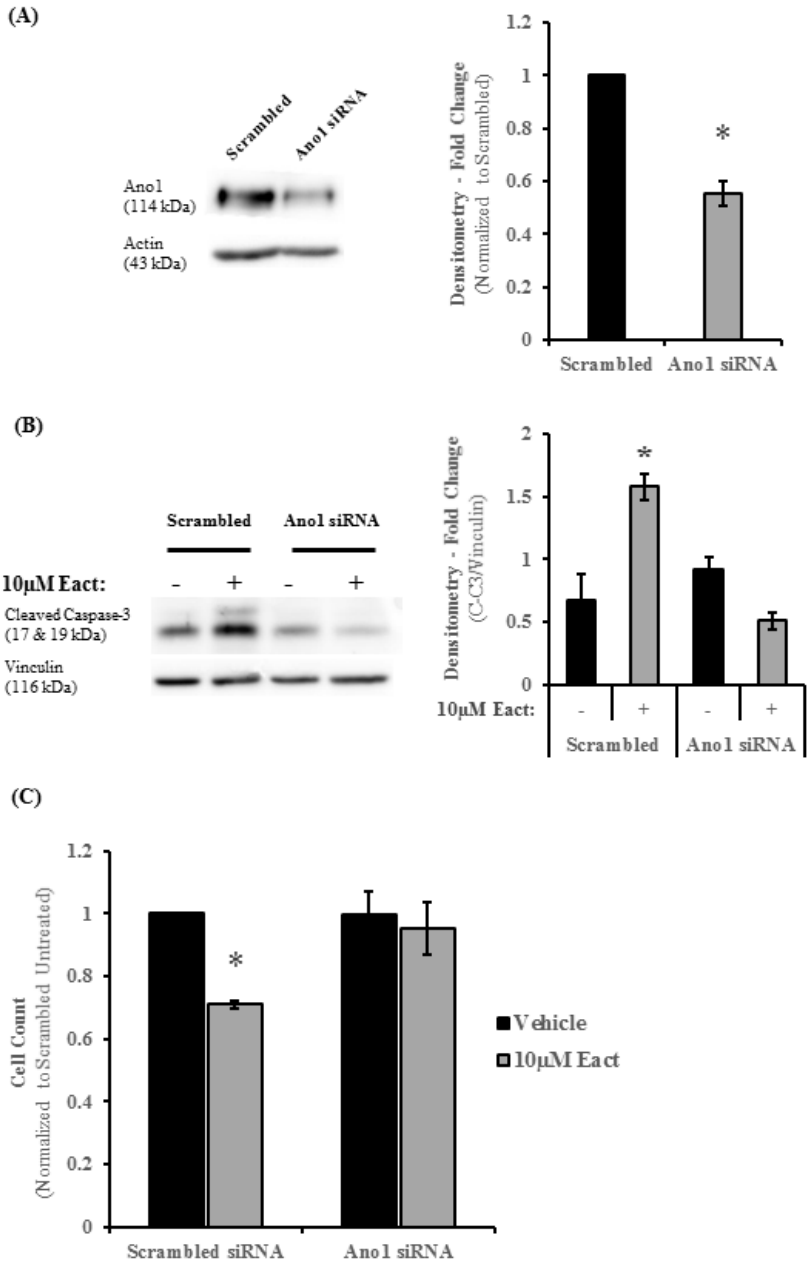

Figure 3: Eact mediates its apoptotic effects via Ano1. **A)** Ano1 expression was evaluated by immunoblot in response to scrambled and Ano1-targeted siRNA knockdown (n = 3, $p < 0.05$). **B)** RLMVECs were transfected with scrambled and Ano1 targeted siRNA and then treated with 10μM Eact or vehicle for 24 hours. Caspase-3 cleavage was then evaluated by immunoblot of treated lysates (n = 3, ANOVA with Tukey Multiple Comparison, $p < 0.05$). **C)** RLMVECs were transfected with scrambled and Ano1 targeted siRNA and then treated with 10μM Eact or vehicle for 24 hours. Alterations of cell number in response to treatments were assessed by cell counts in a haemocytometer (n = 3, ANOVA with Tukey Multiple Comparison, $p < 0.05$).

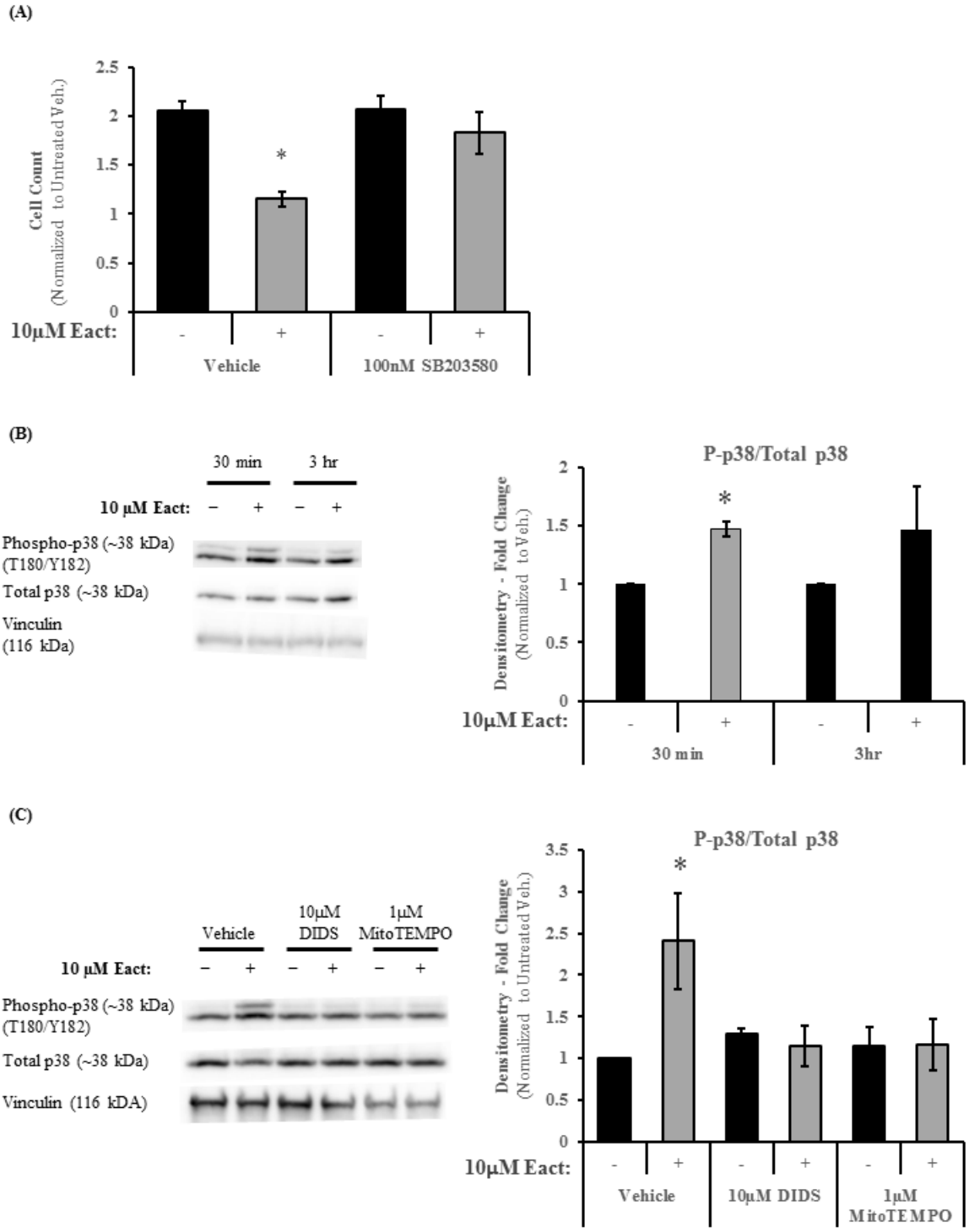
(A)
Cell Count
(Normalized to Untreated Veh.)
2.5
2
1.5
1
0.5
0
*
10μM Eact:
-
+
-
+
Vehicle
100nM SB203580
(B)
30 min
3 hr
10 μM Eact:
–
+
–
+
Phospho-p38 (~38 kDa)
(T180/Y182)
Total p38 (~38 kDa)
Vinculin
(116 kDa)
P-p38/Total p38
Densitometry - Fold Change
(Normalized to Veh.)
2
1.5
1
0.5
0
*
10μM Eact:
-
+
-
+
30 min
3hr
(C)
Vehicle
10μM
DIDS
1μM
MitoTEMPO
10 μM Eact:
–
+
–
+
–
+
Phospho-p38 (~38 kDa)
(T180/Y182)
Total p38 (~38 kDa)
Vinculin (116 kDA)
P-p38/Total p38
Densitometry - Fold Change
(Normalized to Untreated Veh.)
3.5
3
2.5
2
1.5
1
0.5
0
*
10μM Eact:
-
+
-
+
-
+
Vehicle
10μM DIDS
1μM
MitoTEMPO

Figure 4: Ano1 activation increases phosphorylation of p38. **A)** RLMVECs were seeded subconfluently and allowed to adhere before quiescing for 24 hours. Following quiescing, cells were either pre-treated with 100nM SB203580, a specific p38 inhibitor, or vehicle for 1 hour. RLMVECs were then treated with 10µM Eact or vehicle for 24 hours. Changes of cell number in response to treatment were evaluated by cell counts in a haemocytometer ($n = 4$, ANOVA with Tukey Multiple Comparison, $p < 0.05$). **B)** RLMVECs were treated as indicated for 30-minute and 3-hours after which p38 phosphorylation was assessed by immunoblot ($n = 5$, $p < 0.05$). **C)** RLMVECs were pre-treated with either 10µM DIDS, 1µM MitoTEMPO, or vehicle for 1 hour then treated with 10µM Eact for 30 minutes. p38 phosphorylation was then evaluated by immunoblot of treated lysates ($n = 5$, ANOVA with Tukey Multiple Comparison, $p < 0.05$).

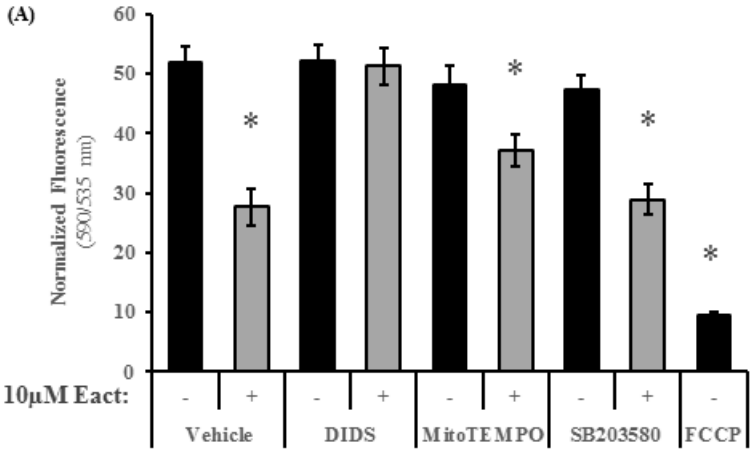
(A)
Normalized Fluorescence (590/535 nm)
60
50
40
30
20
10
0
*
*
*
*
10μM Eact:
-
+
-
+
-
+
-
+
-
Vehicle
DIDS
MitoTEMPO
SB203580
FCCP

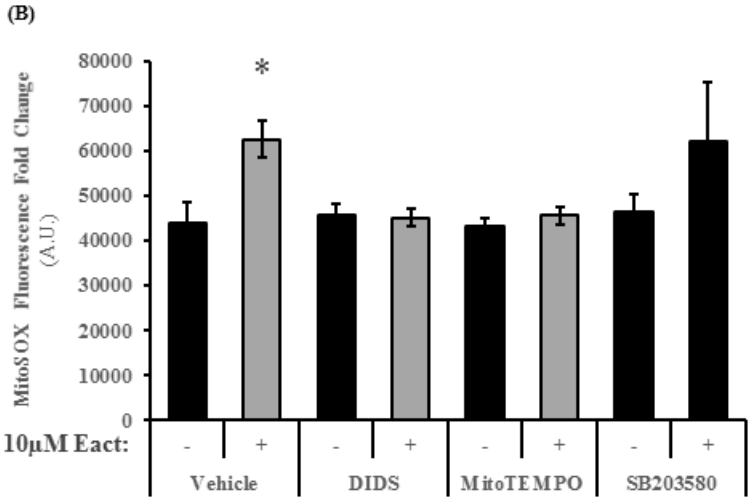
(B)
MitoSOX Fluorescence Fold Change (A.U.)
80000
70000
60000
50000
40000
30000
20000
10000
0
*
10μM Eact:
-
+
-
+
-
+
-
+
Vehicle
DIDS
MitoTEMPO
SB203580

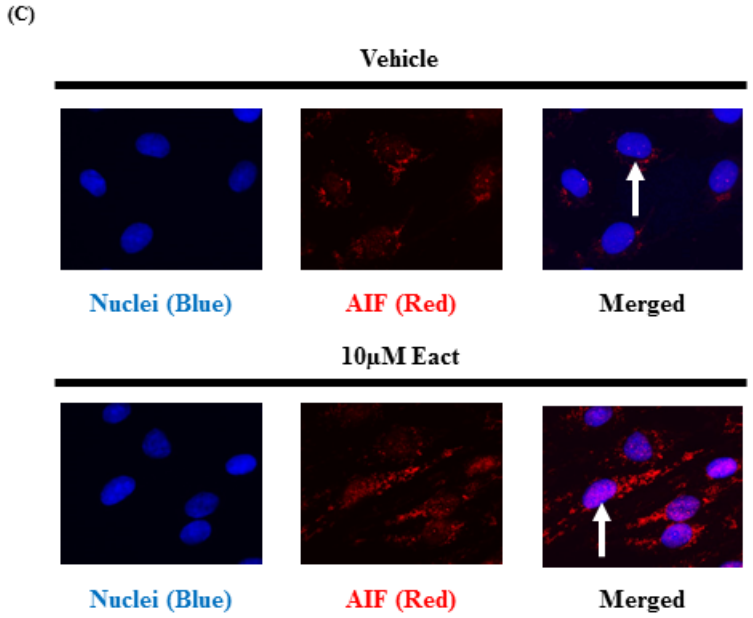
(C)
Vehicle
Nuclei (Blue)
AIF (Red)
Merged
10μM Eact
Nuclei (Blue)
AIF (Red)
Merged

Figure 5: Ano1 activation results in loss of Ψ_m, increased mitochondrial ROS, and AIF nuclear translocation. **A)** RLMVECs were seeded in black 96-well plates and allowed to adhere overnight. Cells were pre-treated with 10µM DIDS, 100nM SB203580, 1µM MitoTEMPO, or vehicle for 1 hour. Cells were then treated with 10µM Eact or vehicle for 20 minutes then loaded with 10µM JC-1 dye for 10 minutes before measuring 528nm (green monomers) and 590nm (red aggregate) fluorescence in a plate reader. ($n = 5$, ANOVA with Tukey Multiple Comparison, $p < 0.05$). **B)** RLMVECs were seeded in black 96-well plates and allowed to adhere overnight. Cells were pre-treated with 10µM DIDS, 100nM SB203580, 1µM MitoTEMPO, or vehicle for 1 hour. Cells were then treated with 10µM Eact or vehicle for 30 minutes then loaded with 5µM MitoSOX for 10 minutes. MitoSOX fluorescence at 590nm was measured in a plate reader setup ($n = 5$, ANOVA with Tukey Multiple Comparison, $p < 0.05$). **C)** Immunofluorescence of AIF was assessed in RLMVECs treated with vehicle or 10µM Eact for 24 hours. Nuclear translocation highlighted with white arrows ($n = 3$).

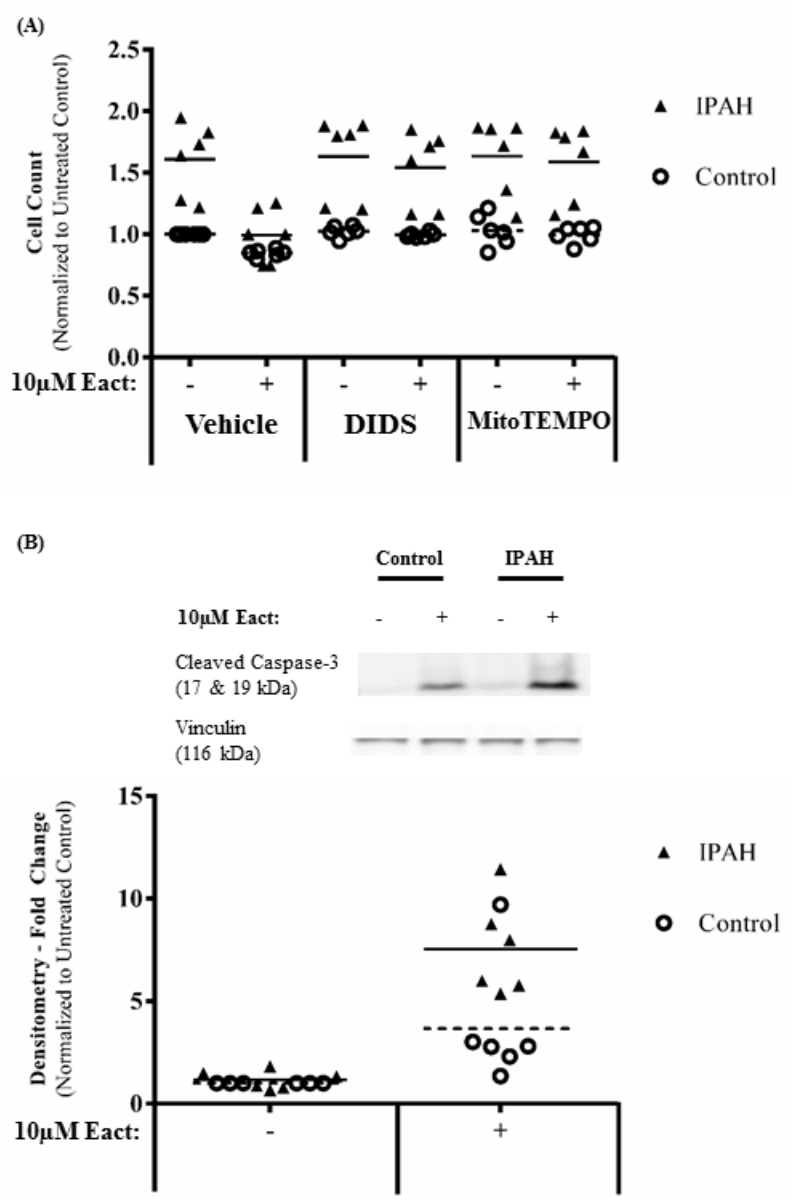

Figure 6: Ano1 activation promotes apoptosis of human IPAH-ECs. **A)** Both control and IPAH ECs isolated from human patient lungs were seeded subconfluently and quiesced. Cells were then pre-treated as indicated for 1 hour, then treated with 10μM Eact in serum-reduced conditions for 24 hours after which cell counts were performed. (n = 2 patients, triplicates) **B)** Immunoblot of cleaved caspase-3 from control and IPAH ECs treated with 10μM Eact or vehicle for 24 hours (n = 2 patients, triplicates).

References

1. Wanitchakool P, Wolf L, Koehl GE, Sirianant L, Schreiber R, Kulkarni S, Duvvuri U, Kunzelmann K. Role of anoctamins in cancer and apoptosis. *Philos Trans R Soc Lond B Biol Sci* 2014;369:20130096.

2. Liu W, Lu M, Liu B, Huang Y, Wang K. Inhibition of Ca2+-activated Cl− channel ANO1/TMEM16A expression suppresses tumor growth and invasiveness in human prostate carcinoma. *Cancer Lett* 2012;326:41–51.

3. Frede J, Fraser SP, Oskay-??zcelik G, Hong Y, Ioana Braicu E, Sehouli J, Gabra H, Djamgoz MBA. Ovarian cancer: Ion channel and aquaporin expression as novel targets of clinical potential. *Eur J Cancer* 2013;49:2331–2344.

4. Duran C, Hartzell HC. Physiological roles and diseases of Tmem16/Anoctamin proteins: are they all chloride channels? *Acta Pharmacol Sin* 2011;32:685–92.

5. Duvvuri U, Shiwarski DJ, Xiao D, Bertrand C, Huang X, Edinger RS, Rock JR, Harfe BD, Henson BJ, Kunzelmann K, Schreiber R, Seethala RS, Egloff AM, Chen X, Lui VW, Grandis JR, Gollin SM. TMEM16A induces MAPK and contributes directly to tumorigenesis and cancer progression. *Cancer Res* 2012;72:3270–3281.

6. Britschgi A, Bill A, Brinkhaus H, Rothwell C, Clay I, Duss S, Rebhan M, Raman P, Guy CT, Wetzel K, George E, Popa MO, Lilley S, Choudhury H, Gosling M, Wang L, Fitzgerald S, Borawski J, Baffoe J, Labow M, Gaither LA, Bentires-Alj M. Calcium-activated chloride channel ANO1 promotes breast cancer progression

by activating EGFR and CAMK signaling. *Proc Natl Acad Sci U S A* 2013;110:E1026–34.

7. Stanich JE, Gibbons SJ, Eisenman ST, Bardsley MR, Rock JR, Harfe BD, Ordög T, Farrugia G. Ano1 as a regulator of proliferation. *AJP Gastrointest Liver Physiol* 2011;301:G1044–G1051.

8. Mazzone A, Eisenman ST, Strege PR, Yao Z, Ordog T, Gibbons SJ, Farrugia G. Inhibition of cell proliferation by a selective inhibitor of the Ca2+-activated Cl- channel, Ano1. *Biochem Biophys Res Commun* 2012;427:248–253.

9. Zhang C-H, Li Y, Zhao W, Lifshitz LM, Li H, Harfe BD, Zhu M-S, ZhuGe R. The Transmembrane Protein 16A Ca 2+ -activated Cl − Channel in Airway Smooth Muscle Contributes to Airway Hyperresponsiveness. *Am J Respir Crit Care Med* 2013;187:374–381.

10. Thomas-Gatewood C, Neeb ZP, Bulley S, Adebiyi A, Bannister JP, Leo MD, Jaggar JH. TMEM16A channels generate Ca2+-activated Cl- currents in cerebral artery smooth muscle cells. *AJP Hear Circ Physiol* 2011;301:H1819–H1827.

11. Yamamura A, Yamamura H, Zeifman A, Yuan JX-J. Activity of Ca2+-activated Cl-- channels contributes to regulating receptor- and store-operated Ca entry in human pulmonary artery smooth muscle cells. *Pulm Circ* 2011;1:269–79.

12. Sun H, Xia Y, Paudel O, Yang X-R, Sham JSK. Chronic hypoxia-induced upregulation of Ca 2+ -activated Cl − channel in pulmonary arterial myocytes: a mechanism contributing to enhanced vasoreactivity. *J Physiol* 2012;590:3507–

3521.

13. Forrest AS, Joyce TC, Huebner ML, Ayon RJ, Wiwchar M, Joyce J, Freitas N, Davis AJ, Ye L, Duan DD, Singer CA, Valencik ML, Greenwood IA, Leblanc N. Increased TMEM16A-encoded calcium-activated chloride channel activity is associated with pulmonary hypertension. *Am J Physiol Cell Physiol* 2012;303:C1229–43.

14. Namkung W, Yao Z, Finkbeiner WE, Verkman a. S. Small-molecule activators of TMEM16A, a calcium-activated chloride channel, stimulate epithelial chloride secretion and intestinal contraction. *FASEB J* 2011;25:4048–4062.

15. Bulley S, Neeb ZP, Burris SK, Bannister JP, Thomas-Gatewood CM, Jangsangthong W, Jaggar JH. TMEM16A/ANO1 channels contribute to the myogenic response in cerebral arteries. *Circ Res* 2012;111:1027–1036.

16. Wang M, Yang H, Zheng LY, Zhang Z, Tang YB, Wang GL, Du YH, Lv XF, Liu J, Zhou JG, Guan YY. Downregulation of TMEM16A calcium-activated chloride channel contributes to cerebrovascular remodeling during hypertension by promoting basilar smooth muscle cell proliferation. *Circulation* 2012;125:697–707.

17. Zhang XH, Zheng B, Yang Z, He M, Yue LY, Zhang RN, Zhang M, Zhang W, Zhang X, Wen JK. TMEM16A and Myocardin Form a Positive Feedback Loop That Is Disrupted by KLF5 During Ang II-Induced Vascular Remodeling. *Hypertension* 2015;66:412–421.

18. Schindelin J, Rueden CT, Hiner MC, Eliceiri KW. The ImageJ ecosystem: An open platform for biomedical image analysis. *Mol Reprod Dev* 2015;in press:DOI: 10.1002/mrd.22489.

19. Comhair SAA, Xu W, Mavrakis L, Aldred MA, Asosingh K, Erzurum SC. Human primary lung endothelial cells in culture. *Am J Respir Cell Mol Biol* 2012;46:723–730.

20. Grinnell K, Duong H, Newton J, Rounds S, Choudhary G, Harrington EO. Heterogeneity in apoptotic responses of microvascular endothelial cells to oxidative stress. *J Cell Physiol* 2012;227:1899–1910.

21. Kunzelmann K, Kongsuphol P, Chootip K, Toledo C, Martins JR, Almaca J, Tian Y, Witzgall R, Ousingsawat J, Schreiber R. Role of the Ca2+-activated Cl- channels bestrophin and anoctamin in epithelial cells. *Biol Chem* 2011;392:125–134.

22. Almaça J, Tian Y, Aldehni F. TMEM16 proteins produce volume-regulated chloride currents that are reduced in mice lacking TMEM16A. *J Biol …* 2009;doi:10.1074/jbc.M109.010074.

23. Picollo A, Malvezzi M, Accardi A. TMEM16 Proteins: Unknown Structure and Confusing Functions. *J Mol Biol* 2015;427:94–105.

24. Zarubin T, Han J. Activation and signaling of the p38 MAP kinase pathway. *Cell Res* 2005;15:11–18.

25. Matsumoto T, Turesson I, Book M, Gerwins P, Claesson-Welsh L. p38 MAP kinase negatively regulates endothelial cell survival, proliferation, and differentiation in FGF-2-stimulated angiogenesis. *J Cell Biol* 2002;156:149–160.

26. Dolado I, Swat A, Ajenjo N, De Vita G, Cuadrado A, Nebreda AR. p38α MAP Kinase as a Sensor of Reactive Oxygen Species in Tumorigenesis. *Cancer Cell* 2007;11:191–205.

27. Tomaskova Z, Ondrias K. Mitochondrial chloride channels - What are they for? *FEBS Lett* 2010;584:2085–2092.

28. Fernández-Salas E, Suh KS, Speransky V V, Bowers WL, Levy JM, Adams T, Pathak KR, Edwards LE, Hayes DD, Cheng C, Steven AC, Weinberg WC, Yuspa SH. mtCLIC/CLIC4, an organellular chloride channel protein, is increased by DNA damage and participates in the apoptotic response to p53. *Mol Cell Biol* 2002;22:3610–20.

Chapter 4

Conclusions and Future Directions

Overview

Our initial objectives for this project were two-fold: 1) we set out to determine Ano1 expression and localization in primary ECs, and 2) with previous studies indicating Ano1 promotes proliferation, we sought to determine whether altering Ano1 activity promoted pulmonary EC proliferation. Activation of Ano1 resulted in apoptosis of rat lung microvascular endothelial cells. Thus, we also sought to determine whether Ano1 could serve as a viable target to attenuate proliferation of PAH ECs.

Conclusions and Future Directions

Chapter 2

Ano1 Expression

We show that Ano1 is expressed in human pulmonary artery endothelial cells (HPAEC) and rat lung microvascular endothelial cells (RLMVEC). More importantly, we also demonstrate that Ano1 expression is significantly elevated both in an animal model of PAH and also from ECs isolated from IPAH patients.

This study is the first to determine that Ano1 is expressed in pulmonary ECs in addition to increased expression in settings of PAH. How Ano1 levels are increased in PAH was not investiated in this study. However, Ano1 expression has been shown to be regulated by STAT6 in response to increases in IL-4 (1). IL-4 levels have been reported to be elevated in PAH (2). Therefore, it is possible that Ano1 levels are increased in PAH in response to increases in IL-4.

It is an important area of investigation to determine how Ano1 levels are regulated in vascular settings and PAH. If Ano1 levels are increasing and causing detrimental effects as some have speculated, then understanding how Ano1 levels are increased would unravel possible strategies to prevent Ano1's adverse effects. On the other hand, we have shown that increased Ano1 expression was not associated with increased proliferation (chapter 3). Instead, we hypothesize that increased Ano1 expression is a reactive response in PAH, perhaps in response to increased inflammation. Further studies are needed to understand the mechanisms underlying increased Ano1 expression in PAH.

Plasmalemmal Ano1

We also confirmed that Ano1 is functional in RLMVEC through measurement of whole cell Ano1 Cl^- currents by patch clamp of RLMVECs. Additionally, we confirmed that activation of Ano1, using a small molecular activator, elicited a significant hyperpolarization of the membrane potential, indicating Cl^- entry into RLMVECs.

The implication of EC membrane hyperpolarization on cell function was not pursued in this project. In general, potassium, chloride, and non-specific cation channels in the endothelium act together to regulate membrane potential (3). In evoking a hyperpolarization in non-excitable cells such as ECs, Ca^{2+} entry can be augmented by increasing the driving force of calcium entry (3). In doing so, activation of Ano1 could result in Ca^{2+} overload of the mitochondria, and thus serve as another apoptotic pathway (4). Further studies will be needed to confirm if this mechanism of apoptosis is also important.

Ca^{2+} entry has also been associated with increased NO production by the Ca^{2+}/CaM/eNOS pathway (5). If alterations in Ano1 activity could alter NO levels, this would provide another avenue for therapeutically targeting Ano1 in PAH as NO and eNOS levels are reduced in PAH patients (6). Furthermore, Ano1 has also been shown to associate with Ezrin/Radixin/Moesin networks, and therefore can play a role in regulating barrier function or EC motility (7, 8) that may be important in inflammation and migration of endothelial cells.

Localization of Ano1 to Mitochondria

The third observation we show in chapter 2 is the localization of Ano1 to RLMVECs mitochondria. This was assessed via confocal microscopy that visually exhibited colocalization of Ano1 to the mitochondria; we also performed subcellular fractionation to demonstrate that Ano1 was not only expressed in the membranous fraction but was prominently enriched in the mitochondrial fraction. This project is the first to indicate that Ano1, a calcium-activated chloride channel, is present in the mitochondria. Further studies are needed to determine whether this can occur different cell types.

Although we believe that our data demonstrating this localization is conclusive, ion channels including chloride channel localization to the mitochondria have consistently been a subject of widespread debate (9). There are also technical difficulties in characterizing the biophysical function of mitochondrial ion channels. Studying the function of Ano1 by patching of mitoplast where the outer mitochondrial membrane (OMM) is stripped would assume that Ano1 is present in the inner mitochondrial membrane (IMM), meanwhile, excised-patch recordings would remove mitochondrial

Ano1 from the rest of the mitochondrial compartments including native ionic concentrations (10). Therefore, before characterizing biophysical properties it is necessary to confirm 1) using Ano1 knockouts that Ano1 is absent from the mitochondria and 2) then whether Ano1 is present in the OMM or IMM. The latter could be done by electron immunogold studies that can determine mitochondrial sub-localization with higher resolution.

Chapter 3

Activation of Ano1 and p38-mediated Caspase-3 Apoptosis

Ano1 activation caused a significant reduction in endothelial cell number which was caspase-3 dependent. Knockdown of Ano1 blocked Eact-mediated apoptosis however, did not reduce cell number of RLMVECs treated with vehicle.

In order to elucidate the upstream mechanism of caspase-3 mediated apoptosis, we first determined via cell count whether p38 inhibition blocked Eact-induced reduction in cell number. p38 inhibition blocked Eact-mediated decreases in cell number. Ano1 activation resulted in a significant increase in p38 phosphorylation. Scavenging mtROS was capable of blocking p38 phosphorylation, suggesting that Ano1 activation caused an increase in mtROS which in turn activated p38.

However, we have not shown whether inhibition of p38 directly inhibited caspase-3 activity. Future experiments will be performed using p38 dominant negative transfection in RLMVECs followed by activation of Ano1. Molecular inhibition of p38 should attenuate Eact-mediated apoptosis. These experiements will allow us to confirm that p38 activity is directly mediating caspase-3 apoptosis.

Functional Role of Mitochondrial Ano1

Due to the localization of Ano1 to the mitochondria we assessed whether alterations in mitochondrial function occurred. Measures of mitochondrial membrane potential ($\Delta\Psi m$) and mtROS were evaluated using JC-1 and MitoSOX respectively. Activation of Ano1 caused a loss of $\Delta\Psi m$ and an increase in mtROS production. We also found AIF was released from the mitochondria during apoptosis and increased nuclear localization. This is the first study to report alterations in mitochondrial function.

As discussed above, mitochondrial sub-localization will provide further insight into how Ano1 is regulating mitochondrial function. This is especially important when considering Ano1's gating mechanism which is dependent on both Ca^{2+} and voltage (11). Hyperpolarized mitochondria would, in theory, keep Ano1 in a closed state, and would only open upon depolarization and presence of Ca^{2+} in the mitochondria. If the mitochondria are depolarized and loaded with Ca^{2+}, then this would allow Ano1 to open. In the opening of Ano1, this would hypothetically allow the mitochondria to re-hyperpolarize. However, very little is known about Cl^- and anion concentrations in the mitochondria to definitively conclude this. Future experiments are needed to evaluate characterize how Ano1's native physiological role.

We have also shown that knockdown of Ano1 using siRNA transfections attenuated Eact-mediated apoptosis. Although we show that we achieved a significant knockdown of Ano1 (~50%), we did not show whether Ano1 expression was reduced in the mitochondrial or plasmalemmal fraction. Therefore, further studies are also necessary to evaluate where siRNA knockdown acted the

Although it was clear that activation of Ano1 caused alterations in mitochondrial function, it remains unclear how Ano1 mediated these changes. Future experiments are needed in order to understand further how Ano1 alters mitochondrial function. This can be done using functional imaging in permeabilized cells (12). Briefly, cells can be gently permeabilized with saponin resulting in uncoupling of the mitochondria from the cell but does not disrupt mitochondrial membranes. Cells can then be loaded with ΔΨm sensitive dyes (e.g. TMRE) or MitoSOX. Mitochondrial Ano1 activation can then be directly studied. In doing so, we can confirm that mitochondrial localized Ano1 directly alters ΔΨm and mitochondrial ROS.

Dissecting the functional role of Ano1 in regulating ΔΨm is not only imperative for the future scope of this study, but can also impact other vascular and cardiovascular settings such as ischemia/reperfusion (I/R) injury. It has been suggested that transient and modest depolarizations of ΔΨm may play a protective role in I/R settings (13). I/R injury is known to result in increased mtROS mediated damage and the role of the mitochondria in mediating these harmful effects is well established (13). However, it has been suggested that modest depolarizations in ΔΨm can dampen the damaging increases in ROS. This is achieved by decreasing the probability of non-specific reduction of oxygen that generate ROS and instead promote electron transfer via the electron transport chain (13). Additionally, depolarization of ΔΨm would decrease the electrochemical driving force for Ca^{2+} overload that is associated with increased ROS and apoptosis (13). While the loss of ΔΨm is undoubtedly linked with intrinsic apoptosis, regulated changes in ΔΨm could be protective in several disease settings. Hence, the role of mitochondrial Ano1 needs to be further investigated.

Implications for Ano1 in PAH

Finally, we assessed whether increased Ano1 expression in IPAH ECs would promote apoptosis. Indeed, Ano1 significantly reduced IPAH EC proliferation when compared to control ECs. This reduction in IPAH EC number was mediated by differentially increasing caspase-3 cleavage in IPAH ECs when compared to control ECs.

It has been established that PAH is a disorder that occurs predominantly in females. However, we have shown that Ano1 levels are elevated in an SUH model of PAH using male Sprague-Dawley rats. Moving forward, we would also be interested in assessing whether Ano1 levels is differentially elevated in a female Sprague-Dawley rats.

Whether elevated Ano1 levels in IPAH ECs contributes to the proliferative phenotype of these cells is unknown. It has been suggested that increased Ano1 expression along with conductance is a requirement for increasing the proliferation of some cancer cell lines (14, 15). If that were the case for PAH ECs, then inhibition of Ano1 would have resulted in decreased cell number. However, here we reported that inhibition using DIDS did not alter cell number. Instead, and somewhat paradoxically, we show that activation of Ano1 is associated with increased apoptosis.

Underlying IPAH EC hyperproliferation is an anti-apoptotic phenotype, where there is an increase in anti-apoptotic members of the BCL-2 family, a shift towards the Warburg effect, and significantly more hyperpolarized mitochondria (16). We hypothesize that the differential apoptosis that Ano1 activation induced in IPAH ECs was mediated by an intrinsic pathway of apoptosis. Additionally, that the increase in Ano1 expression rendered IPAH ECs more susceptible to this activation. We therefore believe

that increased Ano1 does not contribute to the hyperproliferative phenotype of IPAH ECs but rather presents a target to depolarize mitochondria resulting in apoptosis.

We have for the most part utilized a pharmacological approach to study whether activation of Ano1 was capable of inducing apoptosis in pulmonary ECs. Further studies are needed to discern whether inhibition of Ano1 activity could also alter apoptosis. We have shown via siRNA knockdown of Ano1 did not change cell counts when compared to scrambled transfected cells. However, the knockdown only silenced ~50% of protein. Moving forward, further studies need to be performed using viral transfections techniques to knockdown and overexpress Ano1. This approach will allow better transfections efficiencies as pulmonary ECs are difficult to transfect, and allow us to interrogate then Ano1 expression on apoptosis.

A shortcoming of this study is that we have only addressed endothelial cells. As discussed in Chapter 1, the pathogenesis of PAH is not only endothelial in nature, but increased adventitial and smooth muscle cell proliferation is also present (17, 18). Others have reported that Ano1 levels are increased in PASMC from rodent models of PH (19, 20). PASMC proliferation does not only contribute to the pathogenesis of PAH but is also implicated in other groups of PH as well (21). No studies to date have determined if Ano1 could also induce apoptosis of PASMCs. Therefore, future experiments interrogating whether activation of Ano1 in a Sugen-hypoxia model of PAH should be performed. This will allow us to confirm whether Ano1 activation in-vivo would 1) attenuate EC proliferation and 2) if activation of Ano1 could affect other vascular components of the pulmonary vasculature.

References

1. Mazzone A, Gibbons SJ, Bernard CE, Nowsheen S, Middha S, Almada LL, Ordog T, Kendrick ML, Reid Lombardo Km, Shen KR, Galietta LJ V, Fernandez-Zapico ME, Farrugia G. Identification and characterization of a novel promoter for the human ANO1 gene regulated by the transcription factor signal transducer and activator of transcription 6 (STAT6). *FASEB J* 2014;1–12.doi:10.1096/fj.14-258541.

2. Soon E, Holmes AM, Treacy CM, Doughty NJ, Southgate L, MacHado RD, Trembath RC, Jennings S, Barker L, Nicklin P, Walker C, Budd DC, Pepke-Zaba J, Morrell NW. Elevated levels of inflammatory cytokines predict survival in idiopathic and familial pulmonary arterial hypertension. *Circulation* 2010;122:920–927.

3. Nilius B, Droogmans GUY. Ion channels and their functional role in vascular endothelium. *Physiol Rev* 2001;81:1415–1459.

4. Giorgi C, Baldassari F, Bononi A, Bonora M, De Marchi E, Marchi S, Missiroli S, Patergnani S, Rimessi A, Suski JM, Wieckowski MR, Pinton P. Mitochondrial Ca2+ and apoptosis. *Cell Calcium* 2012;52:36–43.

5. Cai H, Liu D, Garcia JGN. CaM Kinase II-dependent pathophysiological signalling in endothelial cells. *Cardiovasc Res* 2008;77:30–34.

6. Humbert M, Morrell NW, Archer SL, Stenmark KR, MacLean MR, Lang IM, Christman BW, Weir EK, Eickelberg O, Voelkel NF, Rabinovitch M. Cellular and molecular pathobiology of pulmonary arterial hypertension. *J Am Coll Cardiol*

2004;43:13S–24S.

7. Perez-Cornejo P, Gokhale a., Duran C, Cui Y, Xiao Q, Hartzell HC, Faundez V. Anoctamin 1 (Tmem16A) Ca2+-activated chloride channel stoichiometrically interacts with an ezrin-radixin-moesin network. *Proc Natl Acad Sci* 2012;109:10376–10381.

8. Adyshev DM, Dudek SM, Moldobaeva N, Kim K -m., Ma S-F, Kasa A, Garcia JGN, Verin AD. Ezrin/radixin/moesin proteins differentially regulate endothelial hyperpermeability after thrombin. *AJP Lung Cell Mol Physiol* 2013;305:L240–L255.

9. O'Rourke B. Mitochondrial ion channels. *Annu Rev Physiol* 2007;69:19–49.

10. Tomaskova Z, Ondrias K. Mitochondrial chloride channels - What are they for? *FEBS Lett* 2010;584:2085–2092.

11. Berg J, Yang HH, Jan LY. Ca2+-activated Cl- channels at a glance. *J Cell Sci* 2012;125:1367–1371.

12. Kuznetsov A V., Mayboroda O, Kunz D, Winkler K, Schubert W, Kunz WS. Functional imaging of mitochondria in saponin-permeabilized mice muscle fibers. *J Cell Biol* 1998;140:1091–1099.

13. Sack MN. Mitochondrial depolarization and the role of uncoupling proteins in ischemia tolerance. *Cardiovasc Res* 2006;72:210–219.

14. Duvvuri U, Shiwarski DJ, Xiao D, Bertrand C, Huang X, Edinger RS, Rock JR, Harfe BD, Henson BJ, Kunzelmann K, Schreiber R, Seethala RS, Egloff AM,

Chen X, Lui VW, Grandis JR, Gollin SM. TMEM16A induces MAPK and contributes directly to tumorigenesis and cancer progression. *Cancer Res* 2012;72:3270–3281.

15. Qu Z, Yao W, Yao R, Liu X, Yu K, Hartzell C. The Ca 2+ -activated Cl − channel, ANO1 (TMEM16A), is a double-edged sword in cell proliferation and tumorigenesis. *Cancer Med* 2014;3:453–461.

16. Masri FA, Xu W, Comhair SA, Asosingh K, Koo M, Vasanji A, Drazba J, Anand-Apte B, Erzurum SC. Hyperproliferative apoptosis-resistant endothelial cells in idiopathic pulmonary arterial hypertension. *Am J Physiol Lung Cell Mol Physiol* 2007;293:L548–54.

17. Paulin R, Michelakis ED. The Metabolic Theory of Pulmonary Arterial Hypertension. *Circ Res* 2014;115:148–164.

18. Stenmark KR, Frid MG, Yeager M, Li M, Riddle S, McKinsey T, El Kasmi KC. Targeting the adventitial microenvironment in pulmonary hypertension: A potential approach to therapy that considers epigenetic change. *Pulm Circ* 2012;2:3–14.

19. Sun H, Xia Y, Paudel O, Yang X-R, Sham JSK. Chronic hypoxia-induced upregulation of Ca 2+ -activated Cl − channel in pulmonary arterial myocytes: a mechanism contributing to enhanced vasoreactivity. *J Physiol* 2012;590:3507–3521.

20. Forrest AS, Joyce TC, Huebner ML, Ayon RJ, Wiwchar M, Joyce J, Freitas N, Davis AJ, Ye L, Duan DD, Singer CA, Valencik ML, Greenwood IA, Leblanc N.

Increased TMEM16A-encoded calcium-activated chloride channel activity is associated with pulmonary hypertension. *Am J Physiol Cell Physiol* 2012;303:C1229–43.

21. Tuder RM, Marecki JC, Richter A, Fijalkowska I, Flores S. Pathology of Pulmonary Hypertension. *Clin Chest Med* 2007;28:23–42.